Center for Integration of Composites into Infrastructure

Evaluating the Performance of Fiber-Based Concrete Mixes for Various Applications

Project Leader: Surya Sarat Chandra Congress
Team: Krishneswar Ramineni, Clay Caldwell

PI: Anand J. Puppala
Professor | A.P. and Florence Wiley Chair
Interim Director – Center for Infrastructure Renewal

Closed Meeting

TAMU Site Proprietary

NSF IUCRC CICI TAMU SITE
NSF IUCRC CICI - IAB Fall 2022 Meeting

December 5-6, 2022

WARSTONE INNOVATIONS, LLC

TEXAS A&M UNIVERSITY
Zachry Department of Civil & Environmental Engineering

Presentation Outline

- Introduction
- Objectives
- Progress of Work
- Laboratory Testing
- Results
- Observations
- Future Work

Introduction

- Climate change and rising seawater levels → huge concerns for coastal areas

- Increase in intensity of storm surges → coastal areas are vulnerable
  - Coastal flooding
  - Shoreline erosion
  - Water pollution
  - High salinity of coastal waters

A neighborhood in Port Arthur, Texas, flooded by Hurricane Harvey in 2017*[a]

Floods from Hurricane Ian, Naples, Florida, USA September 2022*[b]

*Source: SC National Guard [a] , City of Naples FL Police Department [b]

Introduction

- Sandbags are used as barriers to control the destructive behavior of flooding
- Limitations of the current methods
  - Handling and logistical issues
  - Long-term performance of sandbags
  - Limited resources

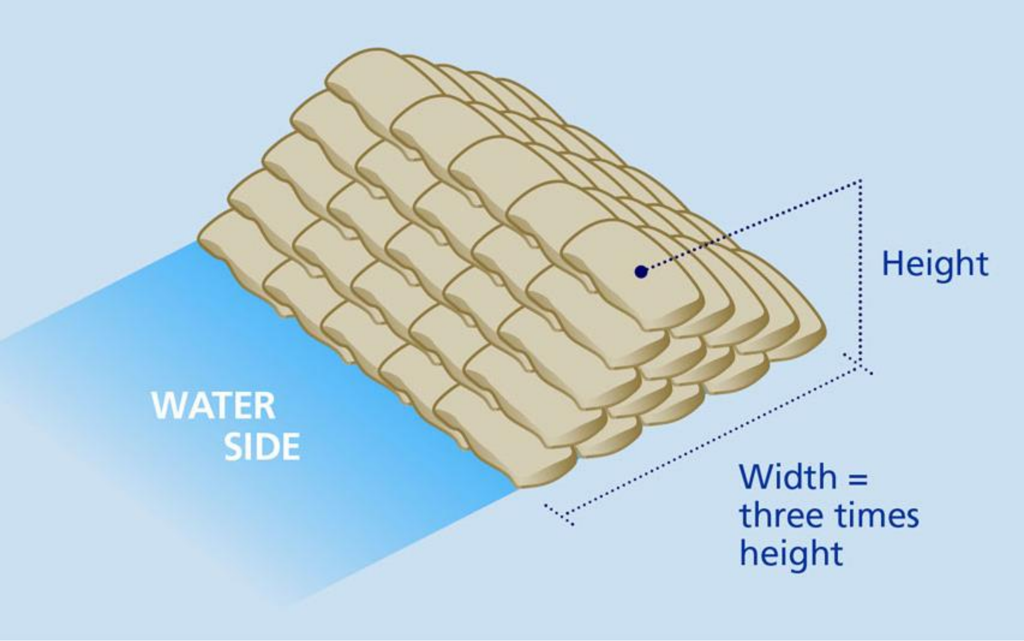

*Source: www.zurich.com

Typical schematic of sandbagging method*

- Objective
  - To develop optimized fiber-based concrete mixes to address the flooding and erosion-related coastal infrastructure problems caused due to climate change

Progress of Work

Task List

- Characterization of materials
- Wetting and Drying studies
  - Potable water (20°C)
  - Seawater (20°C)
  - Varied conditions (40°C and 4°C)
- Permeability studies
- Laboratory-scale large box studies

Last IUCRC meeting
11th May 2022

IUCRC meeting
5th Dec 2022

Laboratory Testing

Concrete mix proportion

Percentage	60%	50%	40%	30%	control
Proportions	1:3:3:10.5	1:3:3:7	1:3:3:4.67	1:3:3:3	1:3:3:0
Cement (g)	86.3	107.8	129.4	151.0	215.7
Sand (g)	322.1	402.6	483.0	563.6	805.2
Pea Gravel (g)	296.2	370.3	444.2	518.4	740.6
Fiber (g)	135.9	113.2	90.6	67.9	0

*Note - Proportions A:B:C:D = Cement: Fine aggregate: Coarse aggregate: Fibers

Concrete mix constituents

Concrete mixes during wetting and drying cycles

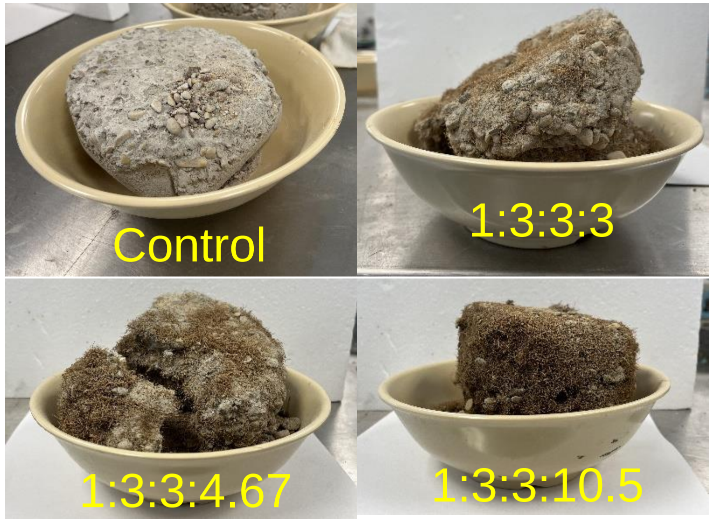

Concrete mixes after five wetting and drying cycles at 20 C

Results - 20°C-50RH-SW

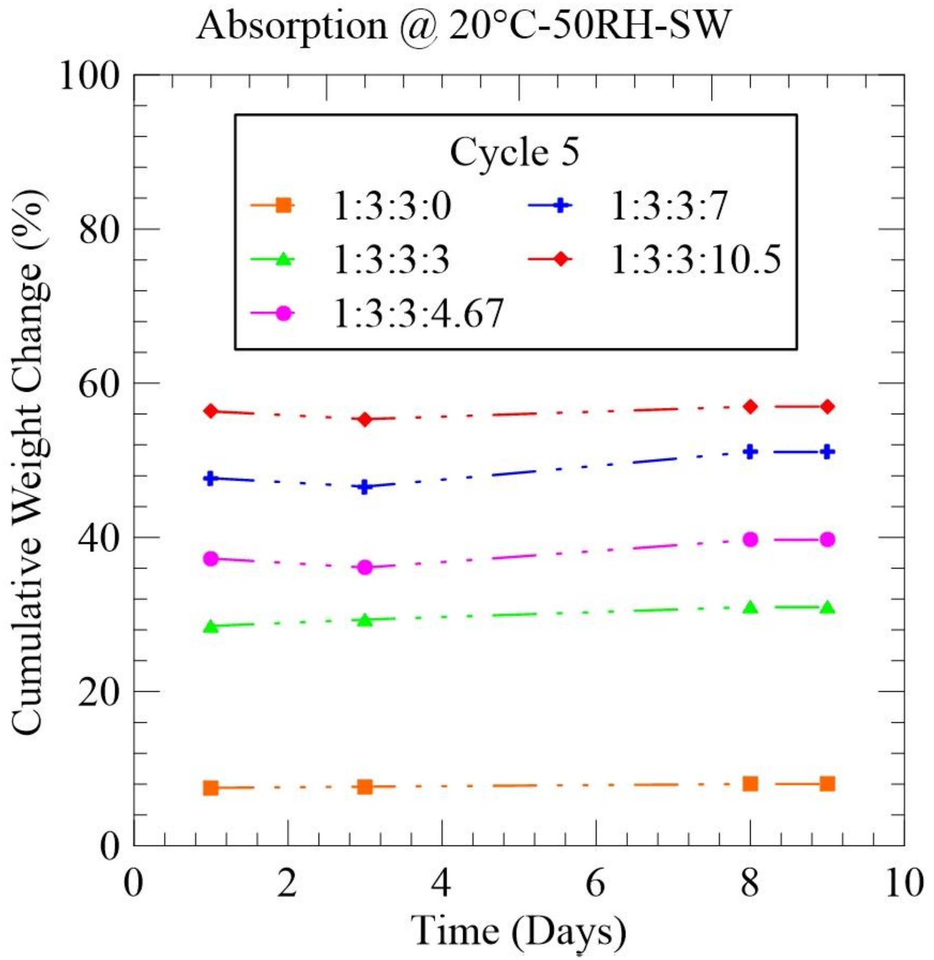

Water absorption vs time for cycle 5

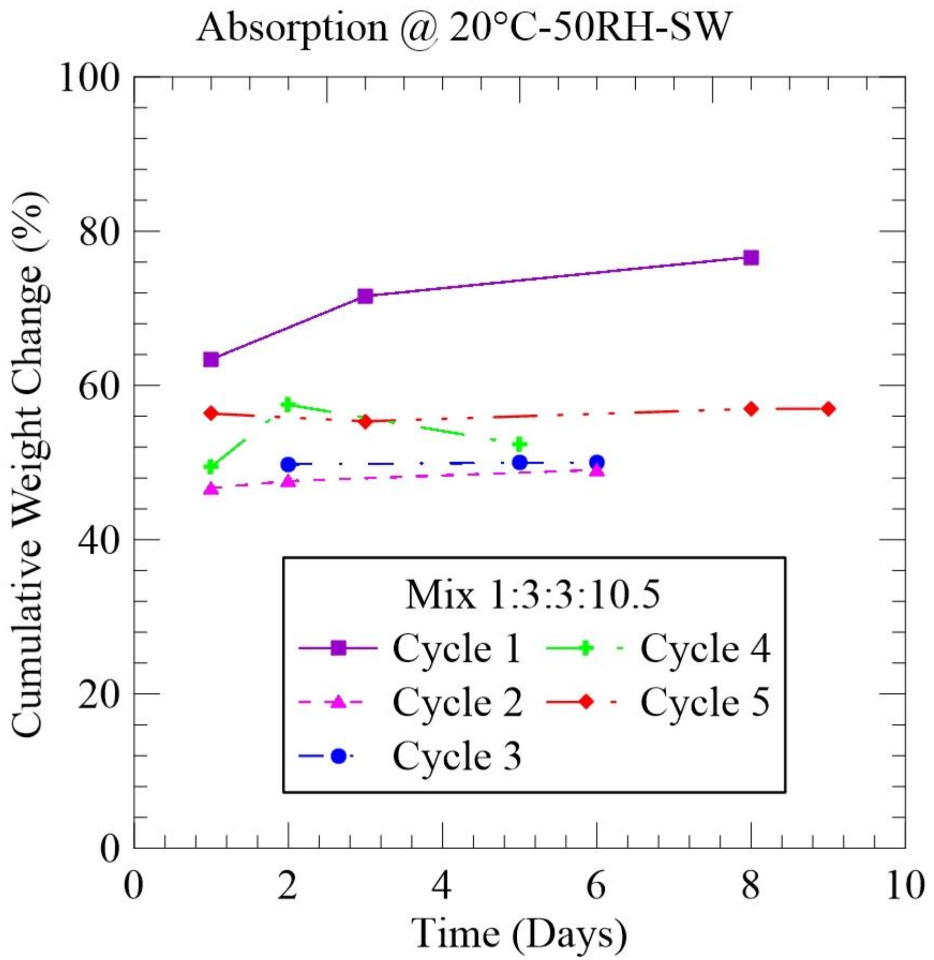

Water absorption vs time for mix 1:3:3:10.5

- ❖ **Fiber dosage ↑→ Water Absorption ↑**
- ❖ **Water absorption after 2 days is constant in all the fiber mixes**

Results - 20°C-50RH-SW

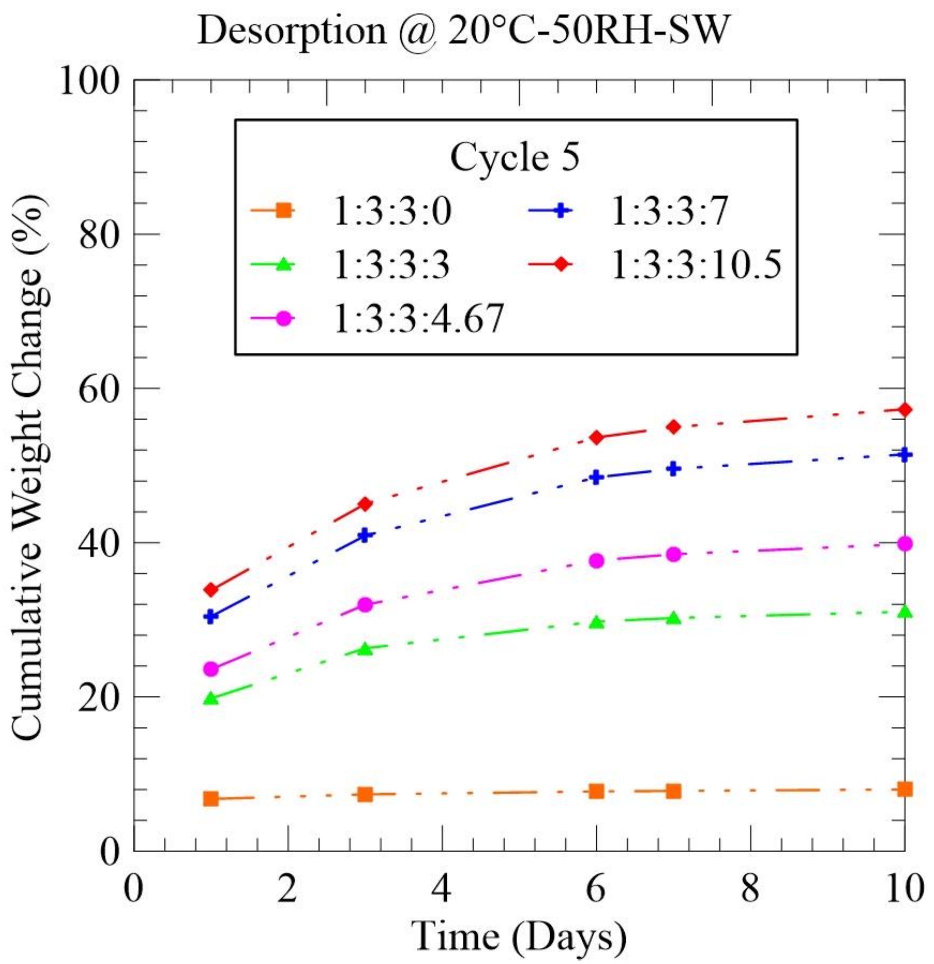

Drying vs time for cycle 5

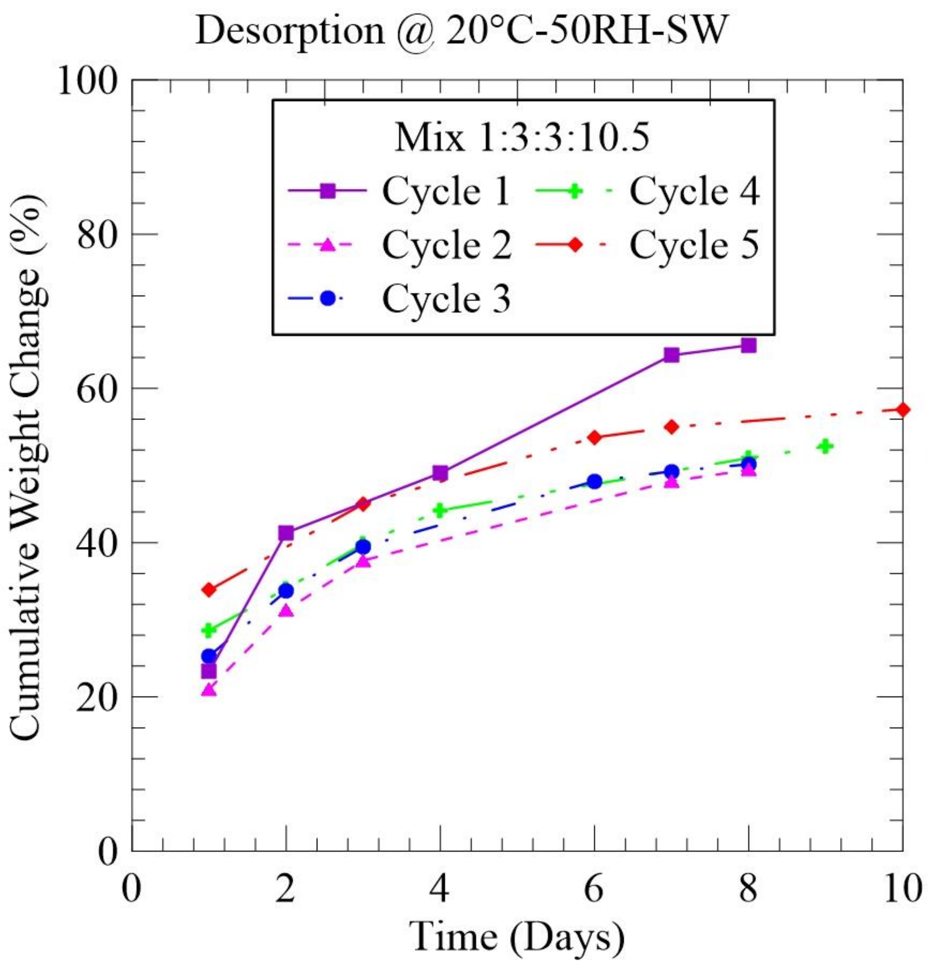

Drying vs time for mix 1:3:3:10.5

- ❖ **Fiber dosage ↑→ Weight change due to drying ↑**
- ❖ **Weight change from drying beyond 8 days is negligible**

Results - 40°C-20RH-PW

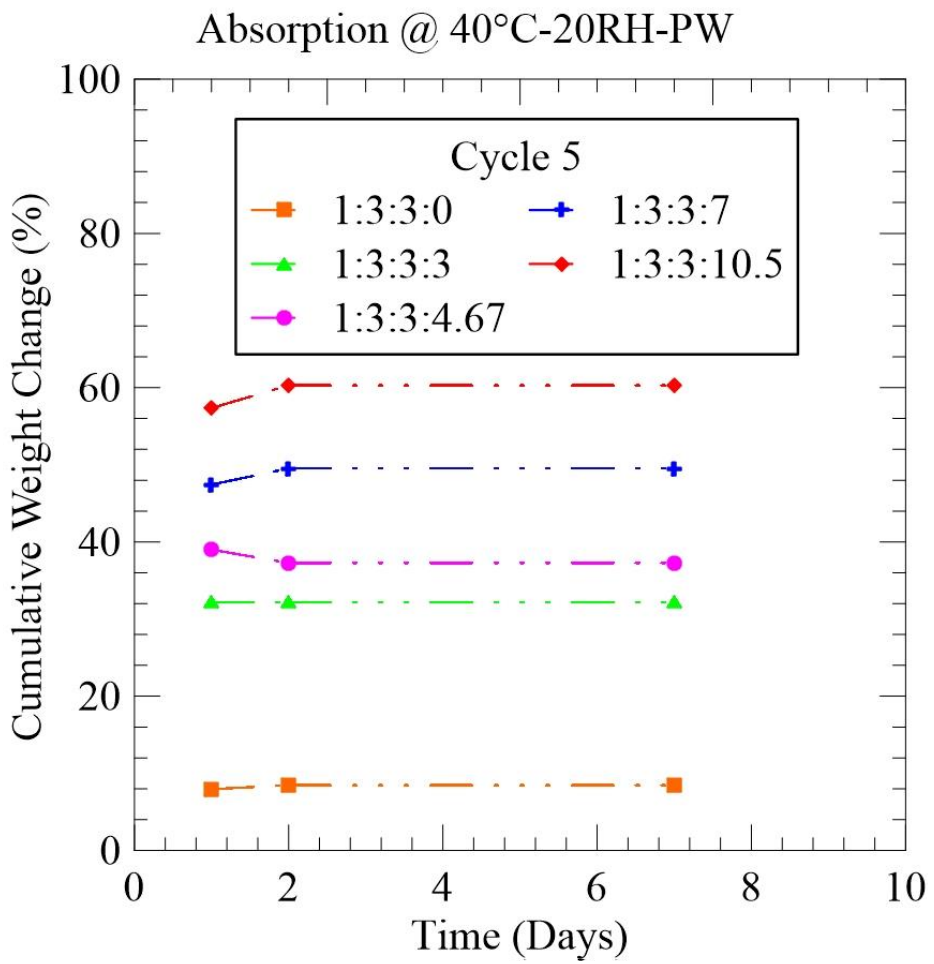

Water absorption vs time for cycle 5

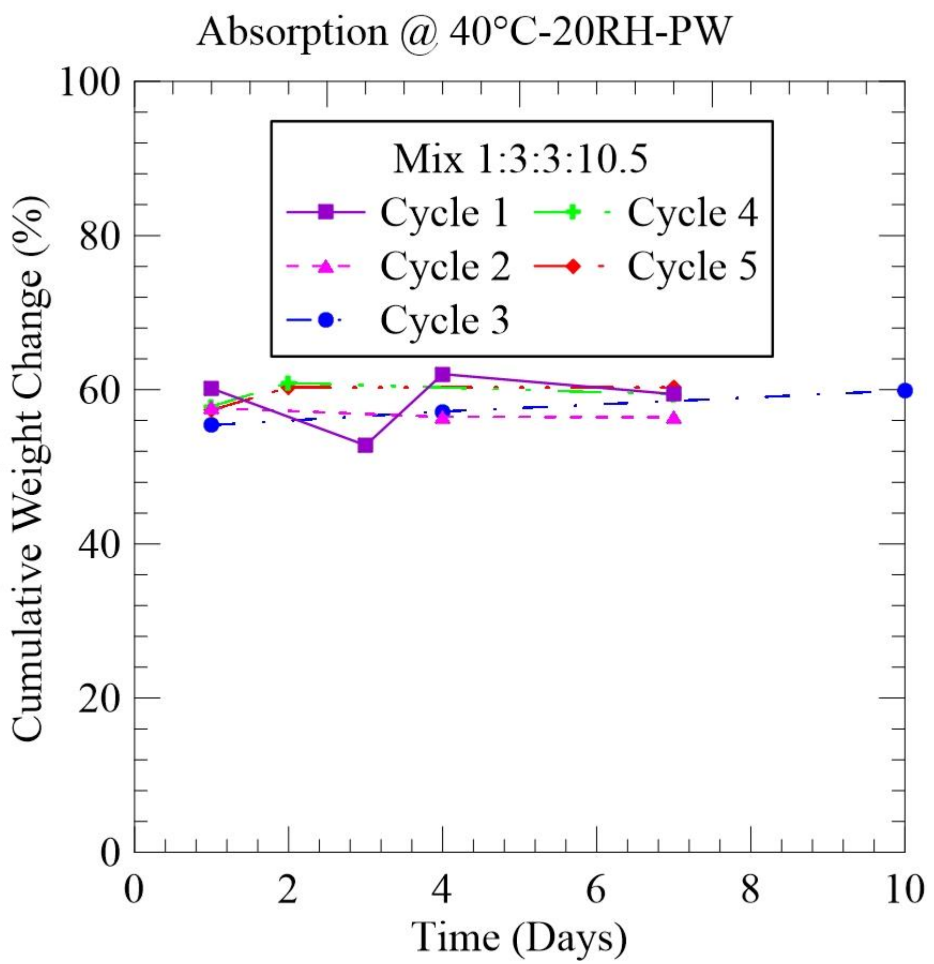

Water absorption vs time for mix 1:3:3:10.5

- ❖ **Fiber dosage ↑→ Water Absorption ↑**
- ❖ **Water absorption after 2 days is constant in all the fiber mixes**

Results - 40°C-20RH-PW

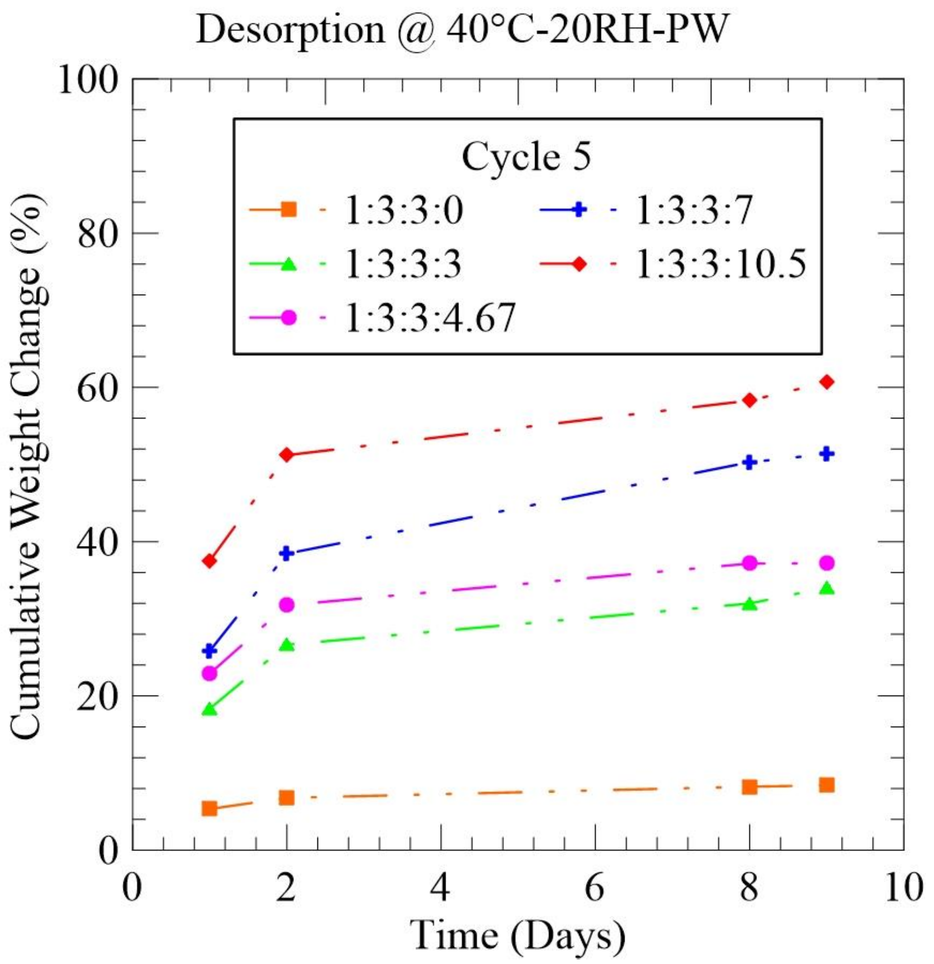

Drying vs time for cycle 5

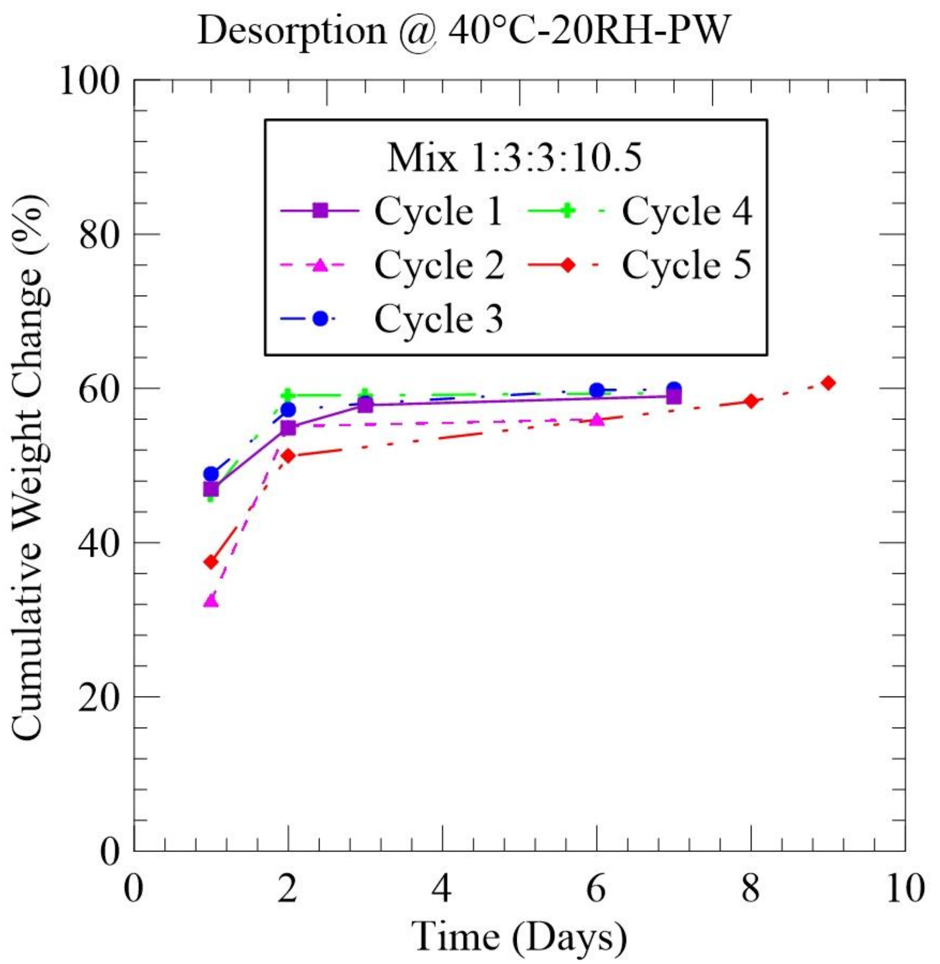

Drying vs time for mix 1:3:3:10.5

- ❖ **Fiber dosage ↑→ Weight change due to drying ↑**
- ❖ **Weight change from drying beyond 4 days is negligible**

Results - 4°C-40RH-PW

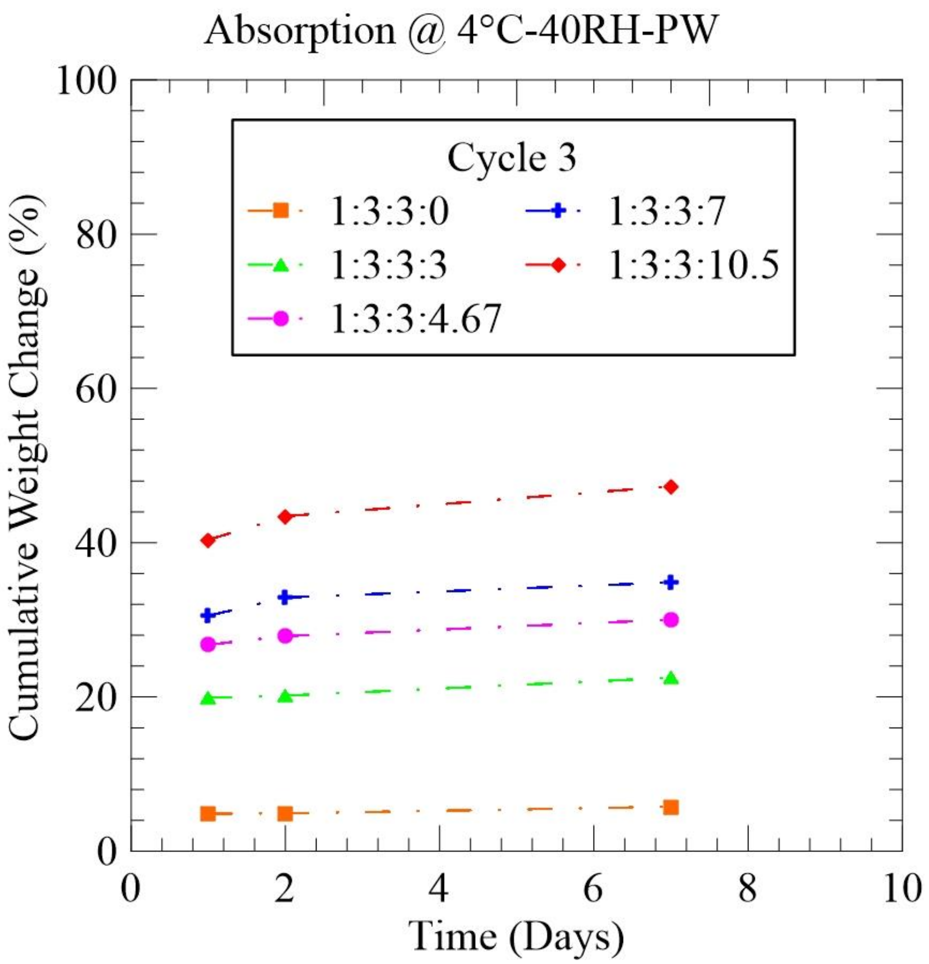

Water absorption vs time for cycle 3

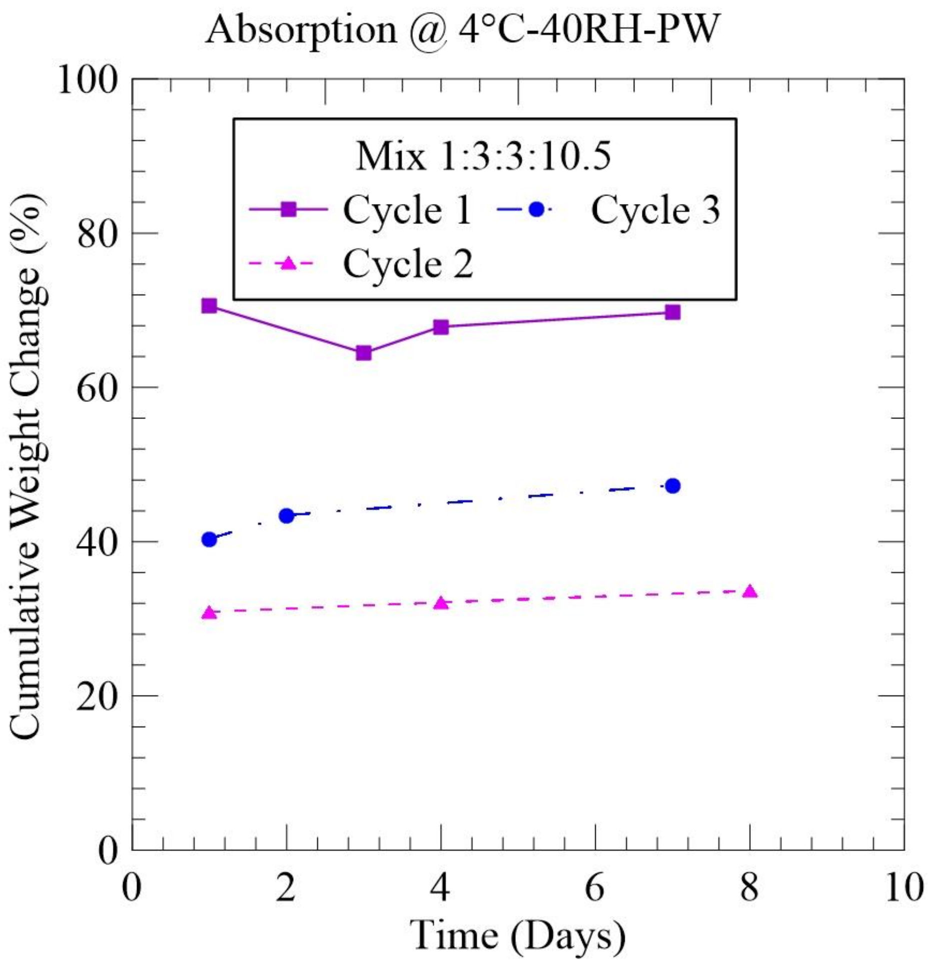

Water absorption vs time for mix 1:3:3:10.5

- ❖ **Fiber dosage ↑→ Water Absorption ↑**
- ❖ **The water absorption after 2 days is constant in all the fiber mixes**

Results - 4°C-40RH-PW

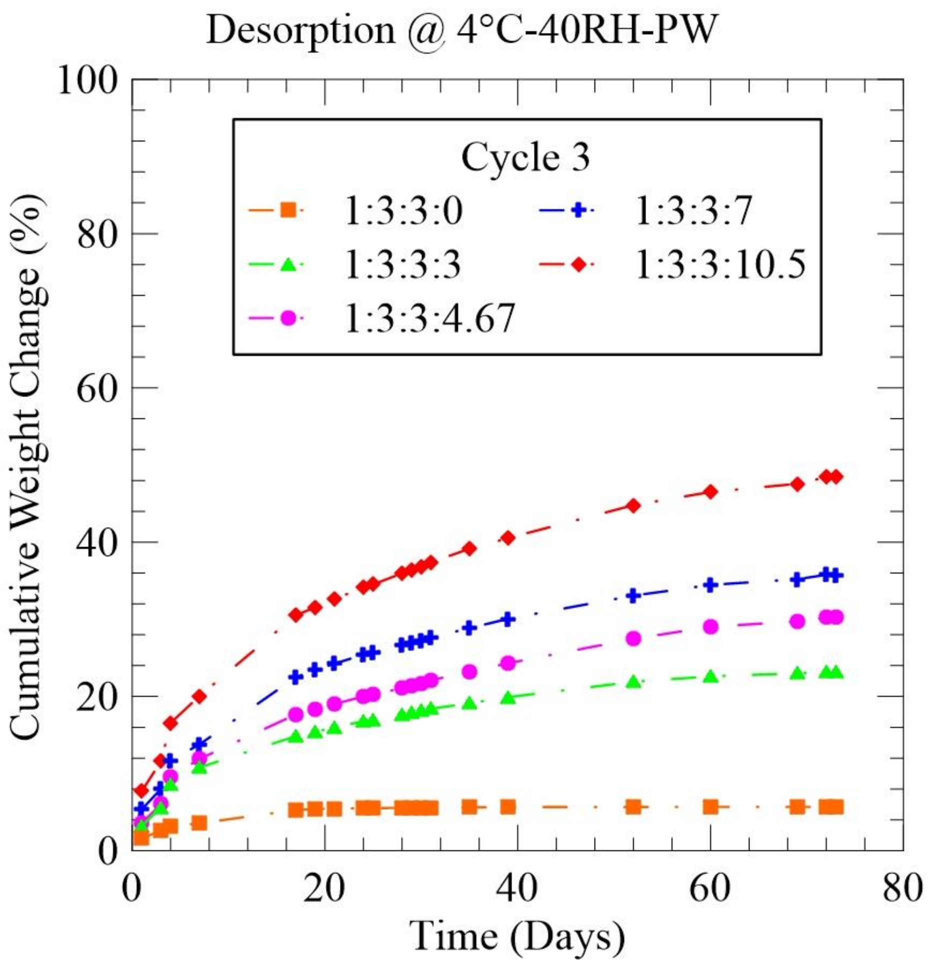

Drying vs time for cycle 3

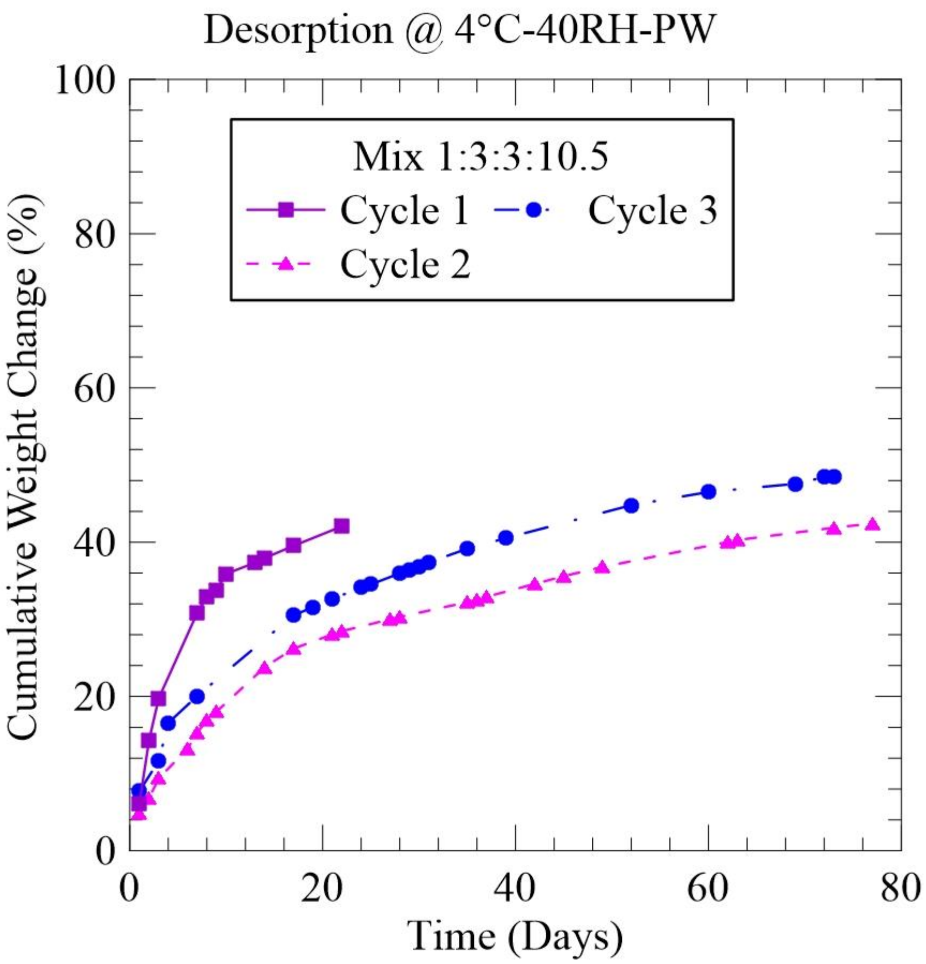

Drying vs time for mix 1:3:3:10.5

- ❖ **Fiber dosage ↑→ Weight change due to drying ↑**
- ❖ **The weight change due to drying after 50 days is negligible**

Summary

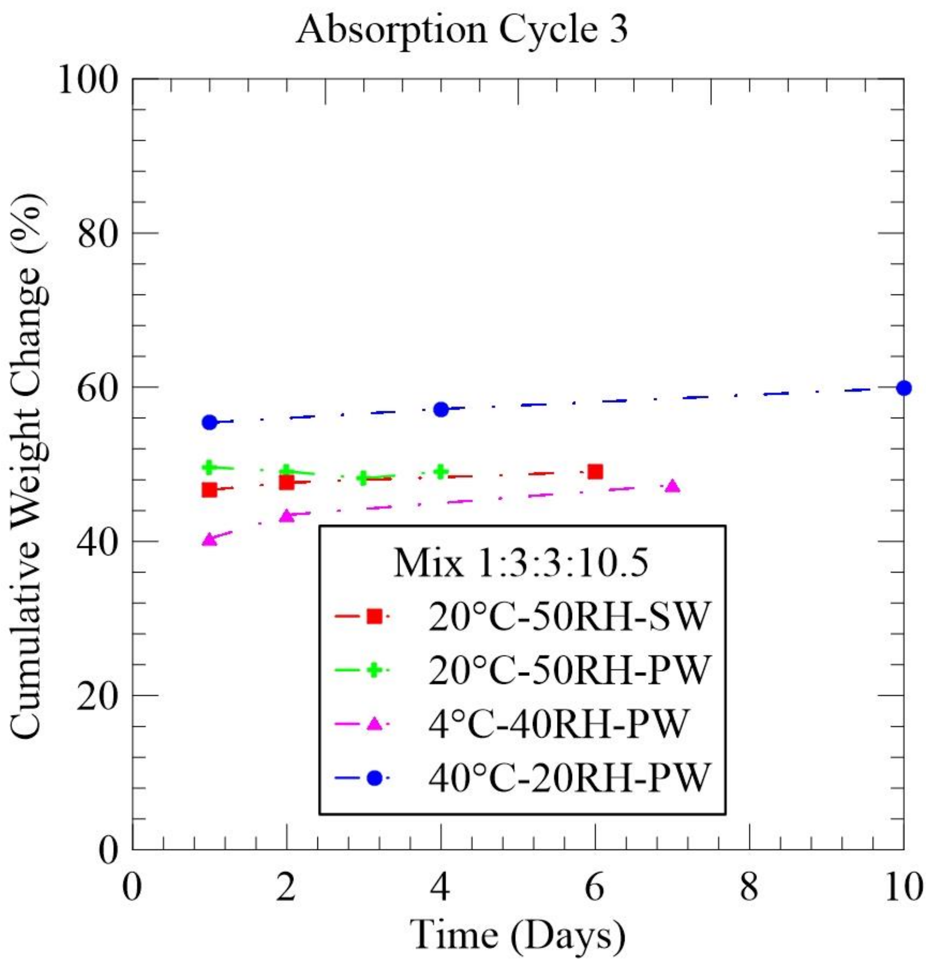

Absorption vs time for cycle 3

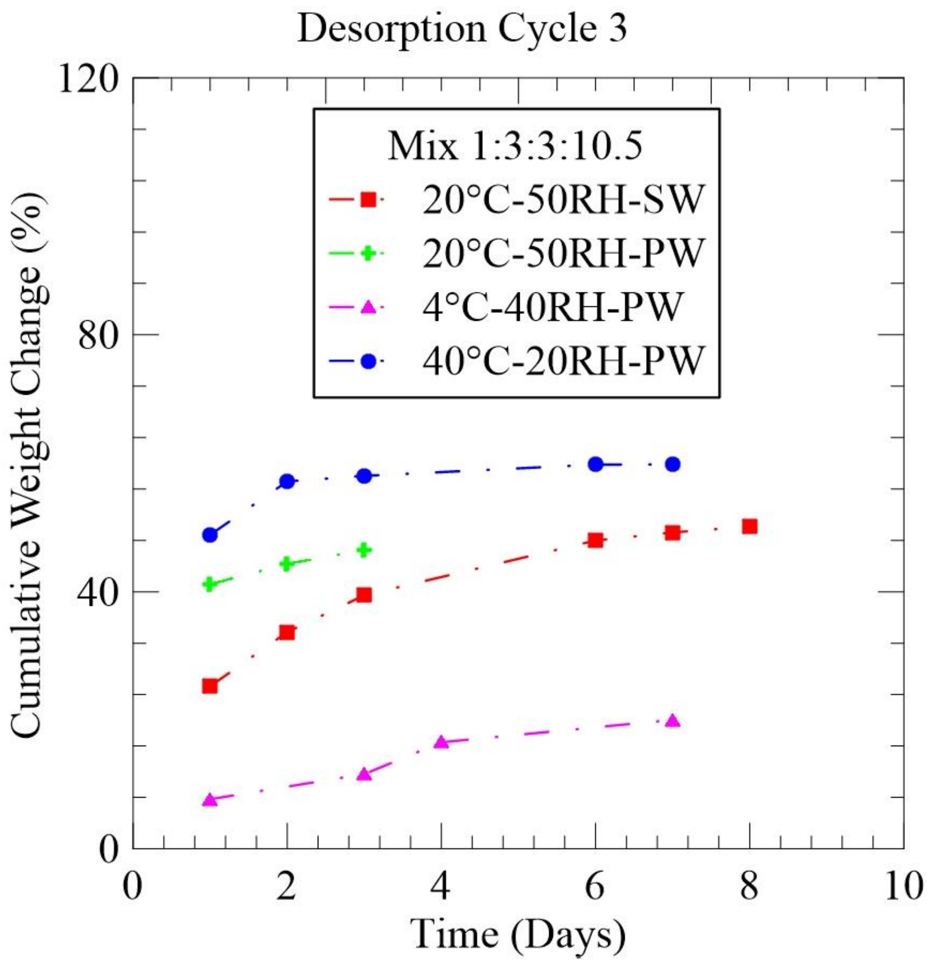

Drying vs time for cycle 3

- ❖ **Temperature and relative humidity have influence**
- ❖ **Saltwater environment → slightly more water retention than portable water**
- ❖ **Environment: 40°C high absorption and desorption**

Observations

- Fiber mixes experienced higher water absorption and desorption (A & D) compared to control mixture
  - Control mix - 1:3:3:0 – Lowest A & D in all testing environments
  - Fiber mix - 1:3:3:10.5 – Highest A & D in all testing environments
- Percent fiber in mixes increases water absorption and desorption
- Time required for concrete mixes to attain equilibrium in both A & D

	20°C-50RH-SW	20°C-50RH-PW	40°C-20RH-PW	4°C-40RH-PW
Absorption	2 days	2 days	2 days	2 days
Desorption	8 days	5 days	4 days	50 days

Future Work

- Permeability studies on optimized mix
- Large scale laboratory testing

LIFE FORMS

Project: Evaluating the Performance of Fiber-Based Concrete Mixes for Various Applications

Number: 5

Center for Integration of Composites into Infrastructure

Application of Geofoam in Thermal Encapsulation of Foundations

Project (Leader): Hiramani R. Chimauriya

Team: Surya S C Congress, Clay Caldwell, Nripojyoti Biswas

PI: Anand J. Puppala

Professor | A.P. and Florence Wiley Chair

Interim Director – Center for Infrastructure Renewal

Closed Meeting

TAMU Site Proprietary

NSF IUCRC CICI TAMU SITE

NSF IUCRC CICI - IAB Fall 2022 Meeting

December 5-6, 2022

ThermaFoam LLC

TEXAS A&M UNIVERSITY

Zachry Department of Civil & Environmental Engineering

Presentation Outline

- Introduction
- Test Methodology
- Control Test (Baseline)
- Geofoam Below Footing (GBF) Tests
  - GBF 8-in. Test
  - GBF 2-in. and 4-in. Tests
- Depth-wise Temperature Profile
- Conclusion
- Future Work

Introduction

- Temperature fluctuations inside the dwellings typically occur from advection, diffusion and radiation at foundation superstructure joints
- About 15% of all heat loss in a home is through floors or basements
- Thermal Encapsulation using Geofoam
  - Research Plan
  - Laboratory Testing Setups

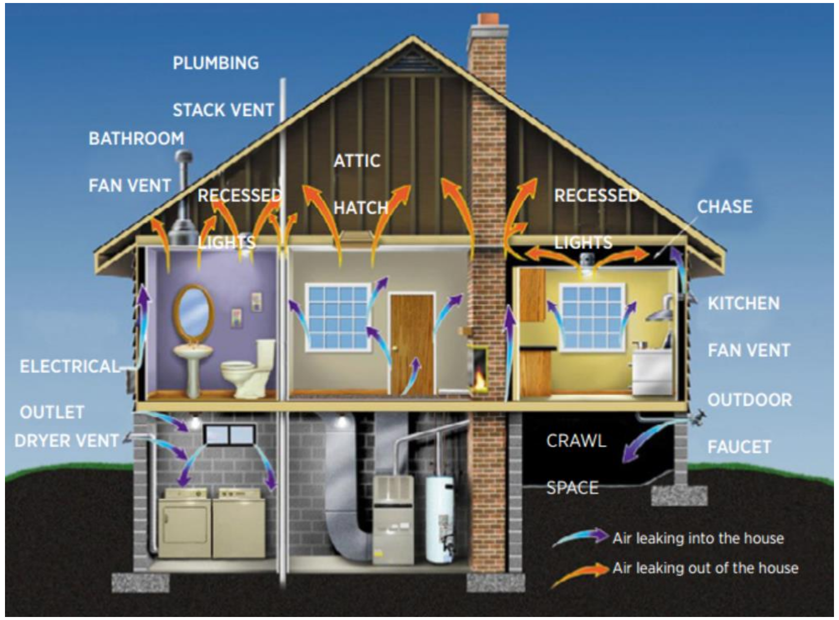

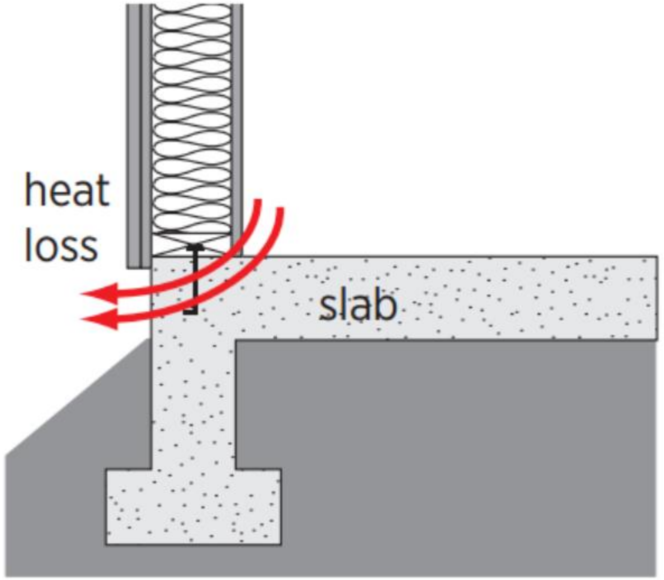

Heat loss

The stack effect

Source: EPA, US DOE (2011, 2012)

Test Methodology

Control Tests (Baseline)

*GBF-8 in. Geofoam-R-250

GBF-4 in. Geofoam-R-250

GBF-2 in. Geofoam-R-250

Repeat set for *GAF

Repeat set for R-100, R-130 and R-150

COMSOL Modeling of Laboratory Tests

Initial Setup

Final Setup

*GBF: Geofoam Below Foundation
GAF: Geofoam Around Foundation

TEXAS A&M UNIVERSITY
Zachry Department of Civil & Environmental Engineering

Control Test (Baseline)

- “Bands” of temperature zones
- Slab-soil interface locations – coldest
- Bottom of the test box – warmest
- Indoor over 2˚C warmer – loss of heat to soil is cooling the slab

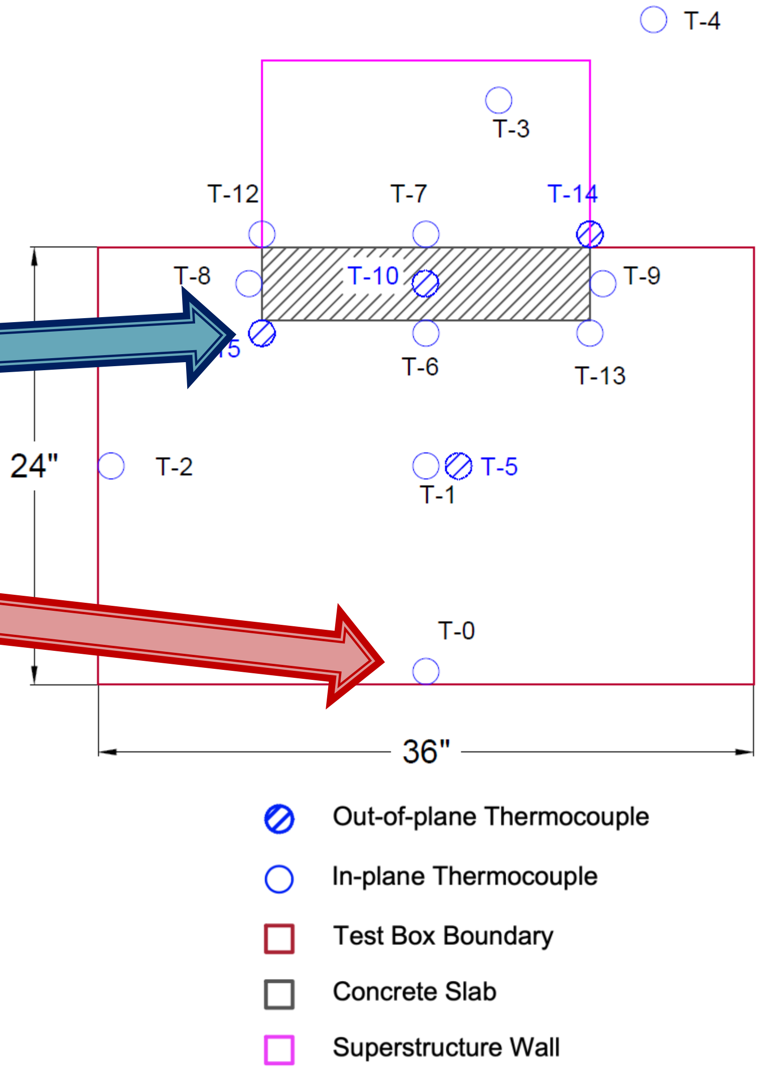

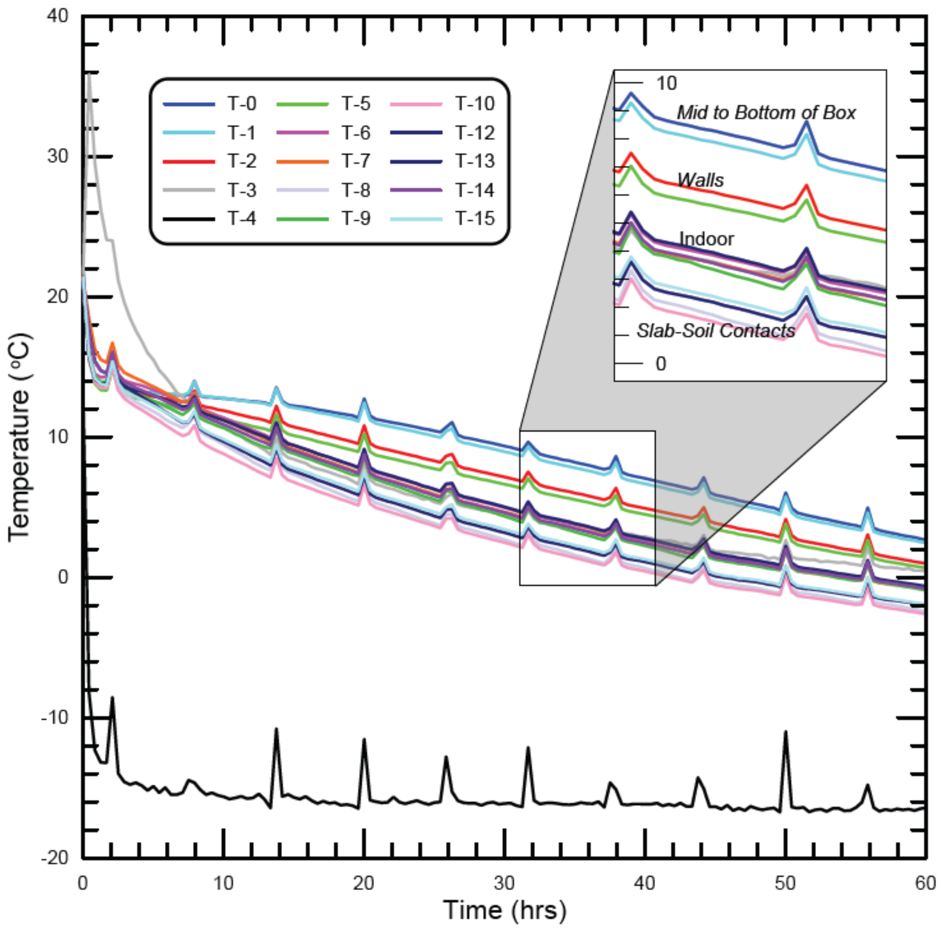

TEXAS A&M UNIVERSITY
Zachry Department of Civil & Environmental Engineering

GBF 8-in. Test

- “Bands” have narrowed
- Bottom of the test box – warmest
- Side walls – coldest
- Indoor and slab temperatures are closer (<1˚C difference) for GBF-8 in. case and warmer than control test – less heat lost to soil
- Geofoam-soil interface warmer than indoor

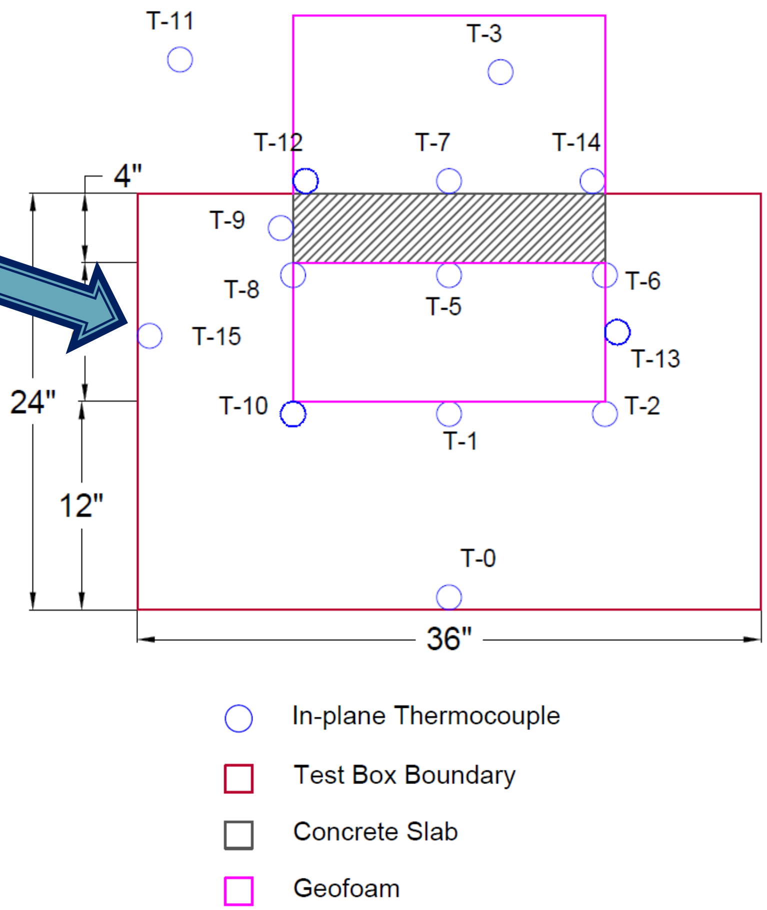

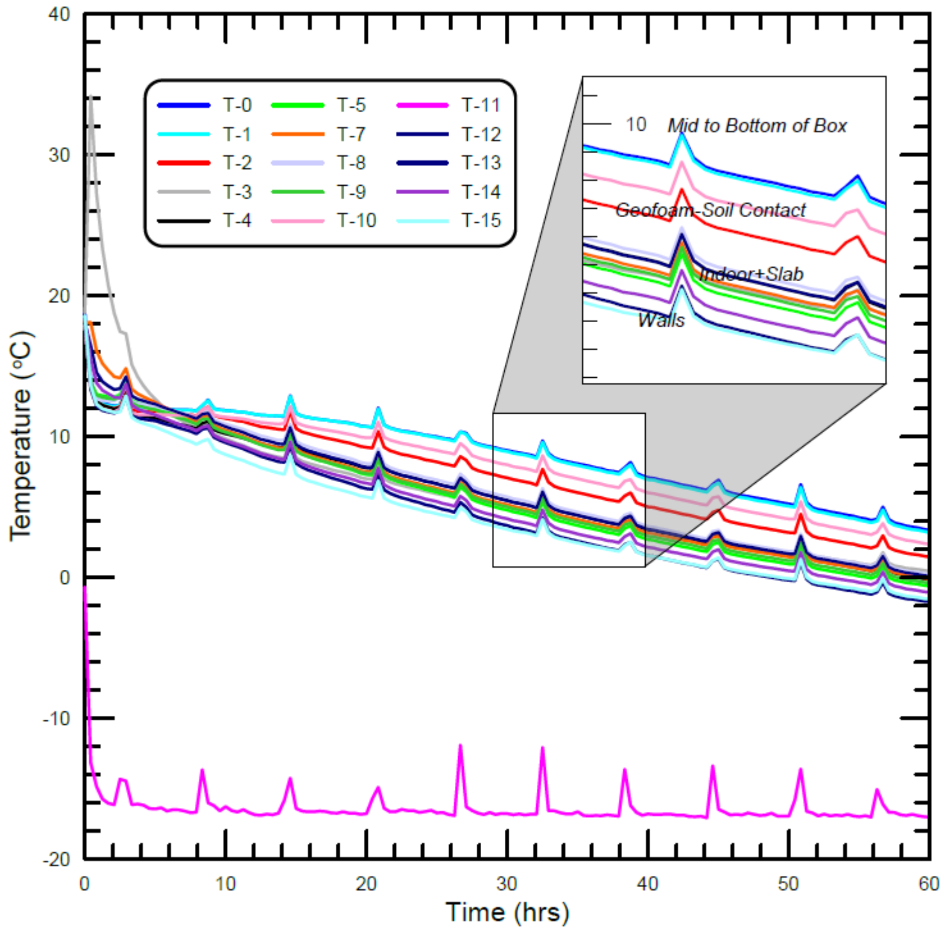

TEXAS A&M UNIVERSITY
Zachry Department of Civil & Environmental Engineering

GBF 2-in. and 4-in. Tests

- Similar trend as 8-in. test observed
- Indoor and slab temperatures for both 2-in. and 4-in. tests are cooler than 8-in. test and closer to control
- Geofoam-soil interface not significantly warmer than indoor for 2-in. test

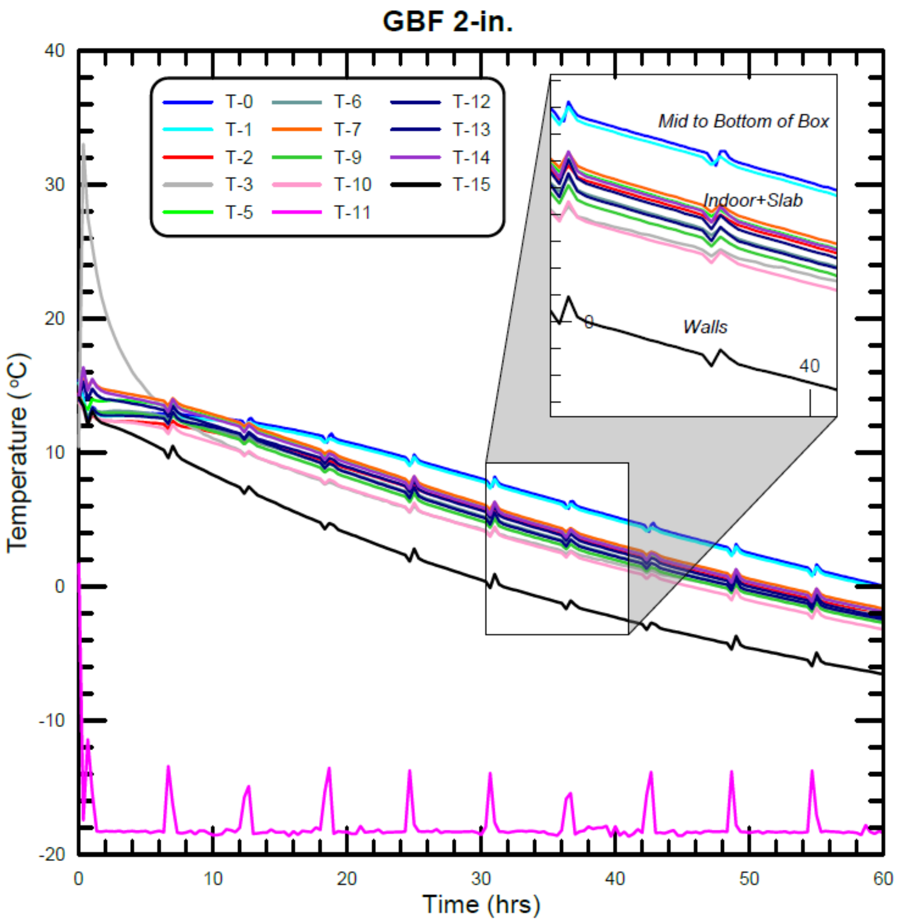

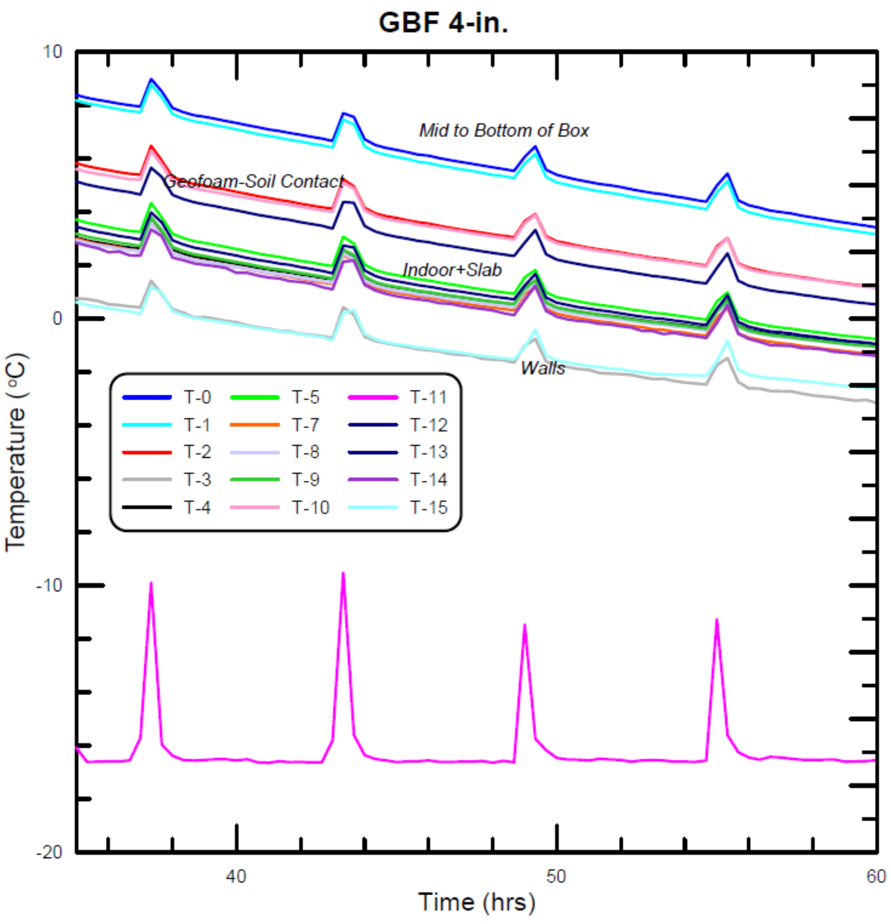

Depth-wise Temperature Profile

- Soil temperature remains almost constant after a certain depth (i.e., a cooler "transient" layer of soil exists)
- Thickness of transient layer is influenced by the presence/ thickness of geofoam
- Heat transfer between soil and slab significantly impeded in this layer, leading to cooler soil temperature (i.e., less heat lost from slab)
- Increased geofoam thickness = Less heat lost to soil

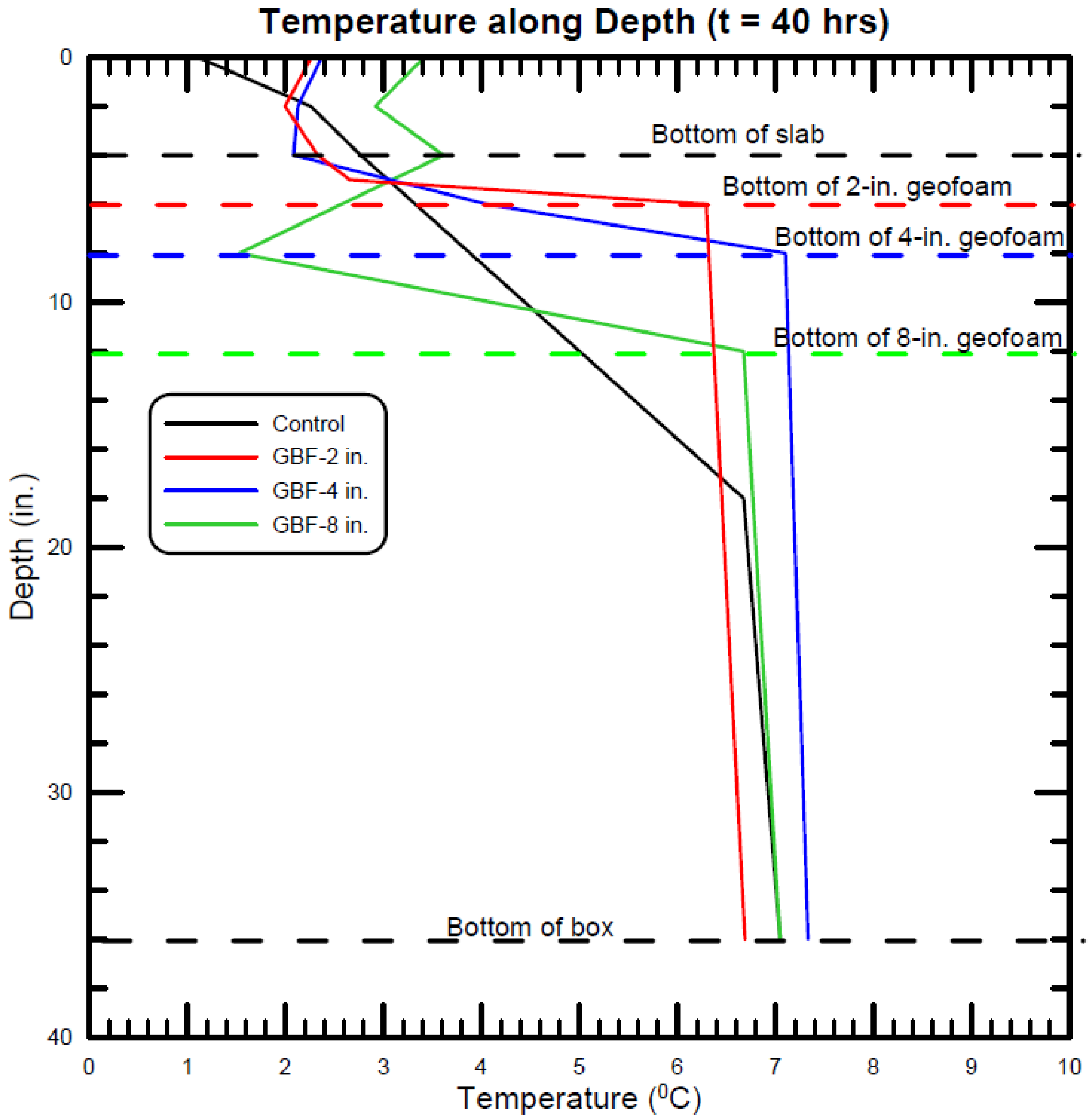

TEXAS A&M UNIVERSITY
Zachry Department of Civil & Environmental Engineering

Conclusions

- Wide variation(>2˚C) in indoor and slab temperature without insulation
- Geofoam insulation reduced this variation in all cases, leading to smaller difference in temperatures and thus lower energy losses
- 8-in. thick geofoam showed best performance with less than 1˚C difference between indoor and slab temperature
- Increased thickness of cooler transient layer with geofoam thickness suggests disruption of heat transfer between soil and slab is a function of geofoam thickness.

Future Works

- Continue lab tests for GAF configuration
- Numerical Simulation of GBF and GAF Tests

LIFE FORMS

Project: Application of Geofoam in Thermal Encapsulation of Foundations

Number: 6

Design and Testing of IFI Geosynthetic Products

Team members: Md Ashrafuzzaman Khan, Krishneswar Ramineni and Clay Caldwell

PI: Anand J. Puppala

Professor | A.P. and Florence Wiley Chair

Director – Center for Infrastructure Renewal

Closed Meeting

TAMU Site Proprietary

NSF IUCRC CICI TAMU SITE

NSF IUCRC CICI - IAB Fall 2022 Meeting

December 5-6, 2022

TEXAS A&M UNIVERSITY

Zachry Department of Civil & Environmental Engineering

Outline of the Presentation

- ❑ Background
- ❑ Objectives and Tasks
- ❑ Working Methodology
- ❑ Material Characterization
- ❑ Large Scale Box Testing
- ❑ Results
- ❑ Summary
- ❑ Future Scope

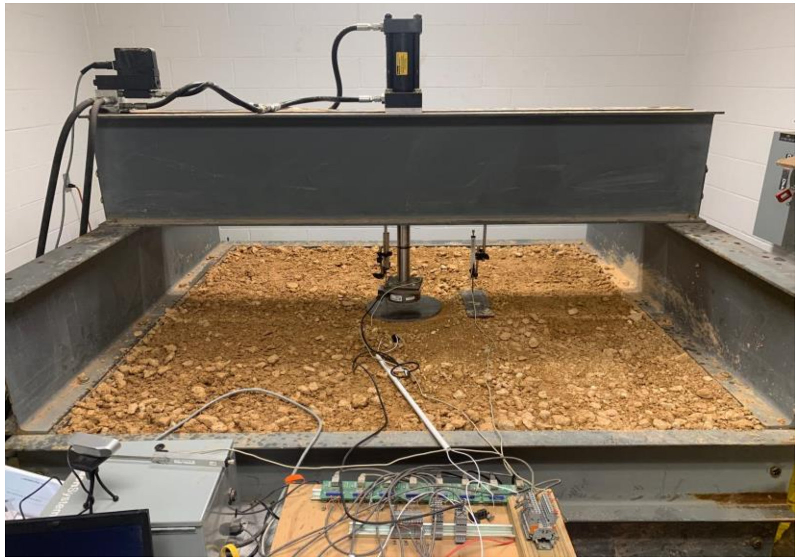

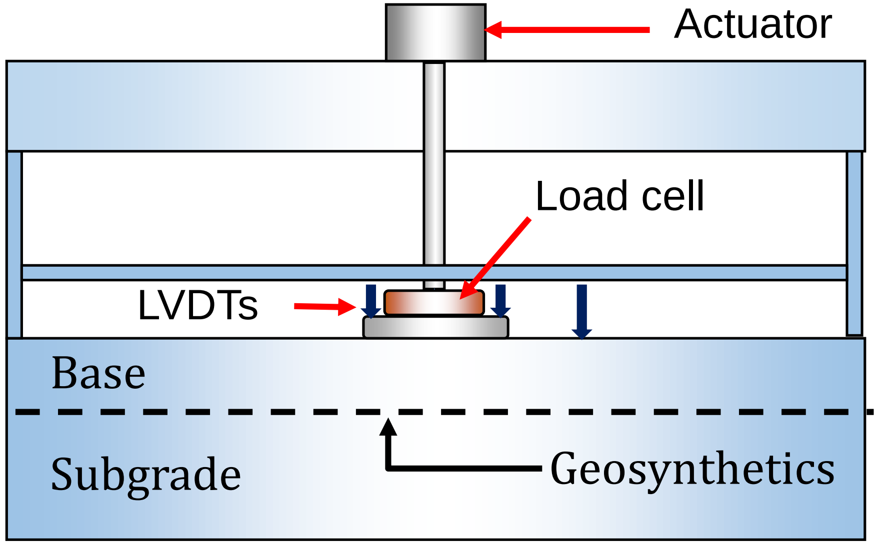

Large-scale Testing Set up (6’ x 6’ x 2.5’)

Background

- ❑ **Existing G-H method is valid up to *j* = 0.8**
- ❑ **The G-H method was based on the experimental study with CBR = 4; however, the design charts were developed within CBR = 1 to CBR = 3**
- ❑ **Need to update the calibration equation and develop design charts to facilitate the flexible pavement design with geocell**

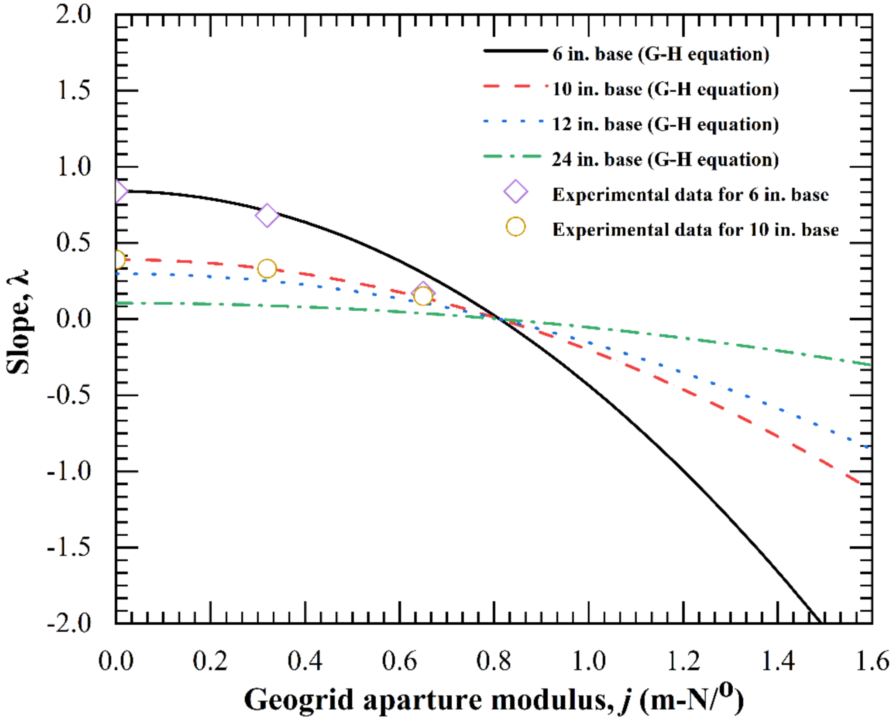

Product ID	Aperture stability m-N/deg.
BL 5	0.80
BL6	0.98
BL7	1.50
FG6 (FAB)	0.98

Objective and Tasks

Research Objective (Part I): Calibrate the existing G-H method for new IFI products

Tasks involved in Part I:

- Material characterization
- Conducting large-scale repeated load tests
- Calibration of G-H method

Research Objective (Part II): Development of various design charts and methods

Tasks involved in Part II:

- Design methods for reinforced unpaved road
- Design methods for reinforced paved road (modified AASHTO)

Working Methodology

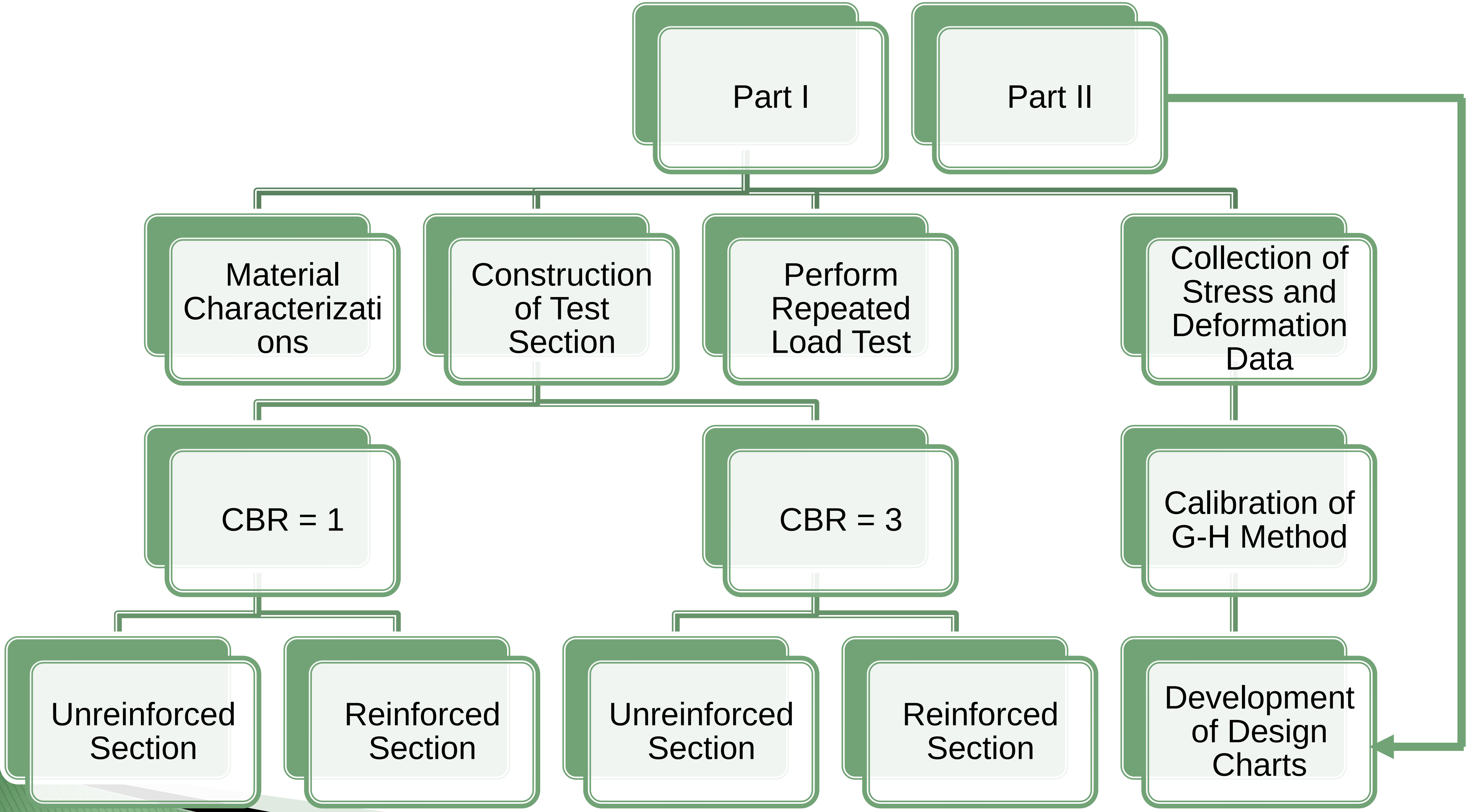

Material Characterizations

- Material Types
  - Soil
    - Grain-size
    - Standard Proctor
    - Atterberg limit
    - CBR
    - LWD-CBR
  - Unbound Aggregates
    - Grain-size
    - Standard Proctor
    - Atterberg limit
    - CBR
  - Geosynthetics
    - Source: IFI

CBR for Subgrade

Test No.	MC (%)	CBR
1	5.0	10
2	**9.2**	**3.0**
3	10.0	2.6
4	**12.5**	**1.0**
5	15.0	0.9

CBR for Base

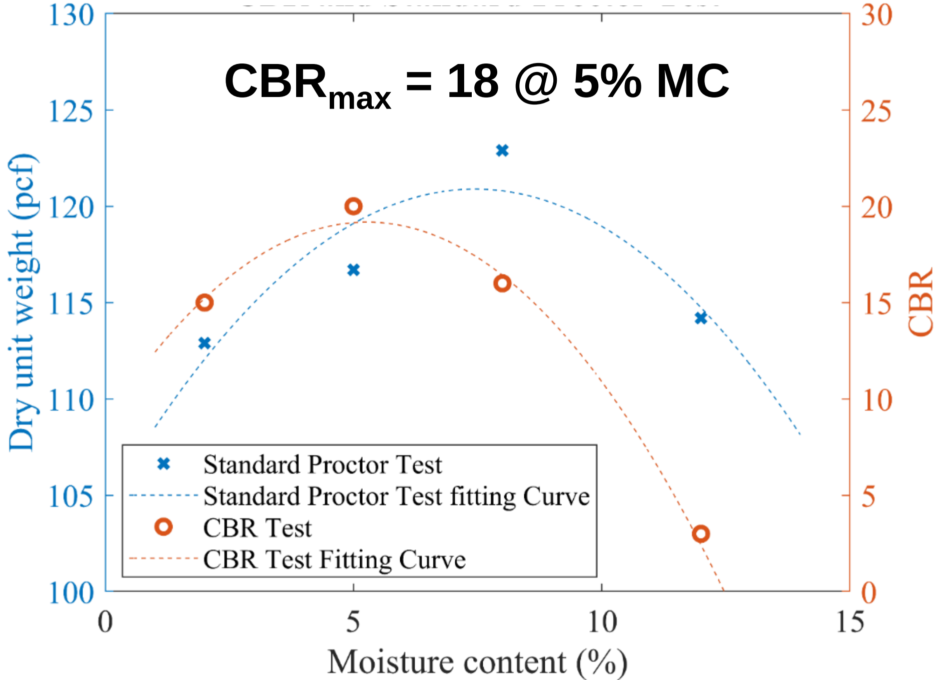

Large-scale Box Testing
Testing Plan

Table : Large-Scale Cyclic Plate Load Testing Plan Note: UR- Unreinforced; GG- Geogrid; GC- Geocell; FG- Fabgrid					
Testing Sequence	Test Designation	Geosynthetic type	Subgrade Soil: CBR value	Number of tests as per plan	Remarks
1	Unreinforced (Control)	-	1 & 3	2	**Completed (4 additional)**
2a	FG	Fabgrid (FG6)	1 & 3	2	**Completed**
2b	GG	Geogrid (BL5, BL6, BL7)	1 & 3	6	**Completed**
3a	GC	Geocell (4 in.)	1 & 3	2	**CBR=1 completed, CBR = 3 completed**
3b	GC	Geocell (6 in.)	1 & 3	2	**CBR=1 completed, CBR = 3 completed**
4a	GG:GC	Geocell (4 in.) + BL6	1 & 3	2	**CBR=1 completed, CBR = 3 completed**
4b	GG:GC	Geocell (6 in.) + BL6	1 & 3	2	**CBR=1 completed, CBR = 3 completed**
Total number of testing:				18	

Large-scale Box Testing

Testing Parameters

- Reinforcement were placed at the interface of base and subgrade layer
- Main objective of the repeated load testing was to determine the load distribution angles with the number of loading cycles

$$h = \frac{r}{\tan\alpha}\left(\sqrt{\frac{P}{\pi r^2 p_i}} - 1\right)$$

p_i = normal stress at the interface of base and subgrade layer (kPa)
P = wheel load (KN)
r = radius of the equivalent tire contact area (m)
h = thickness of the base layer (m)
α = stress distribution angle

$$\frac{1}{\tan\alpha} = \frac{1}{\tan\alpha_1} + \lambda^* \log N$$

α = stress distribution angle for the case where the number of passes is N;

α_1 = stress distribution angle for the case where the number of passes is one

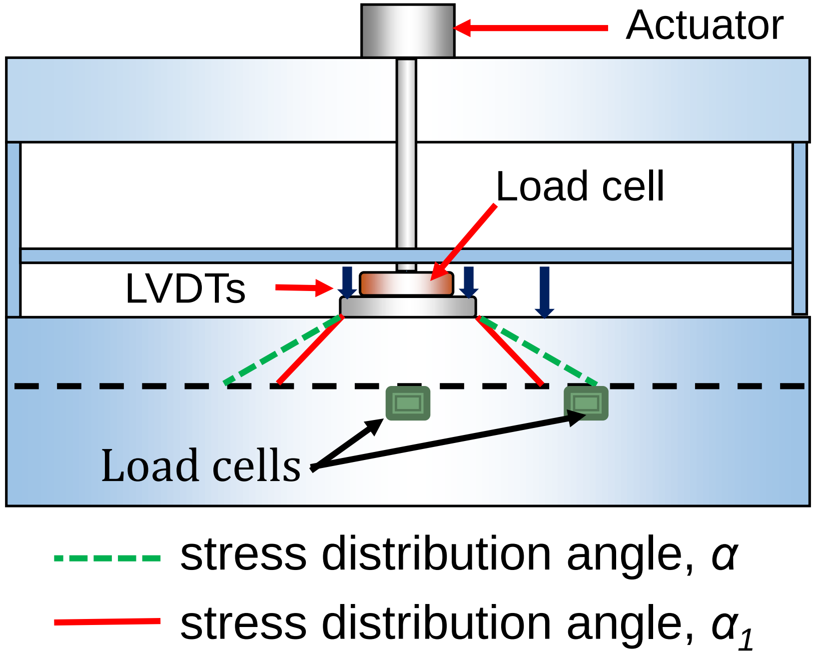

Results

Geogrids (CBR = 1)

- ❑ **Aperture stability modulus of geogrids: BL5 < BL6 < BL7**
- ❑ **Maximum permanent deformation (PD) after 5000 cycles: BL5 > BL6 > BL7**
- ❑ **PD of (BL6 + Geotextile) < FG6 → interaction with aggregates**

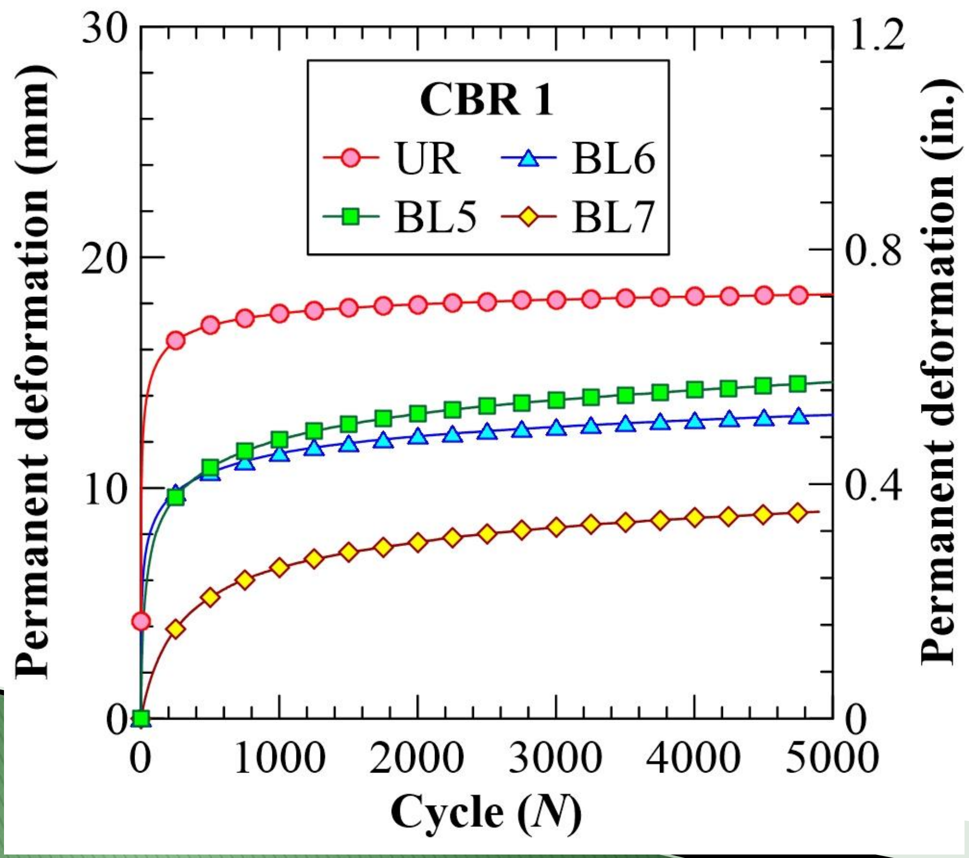

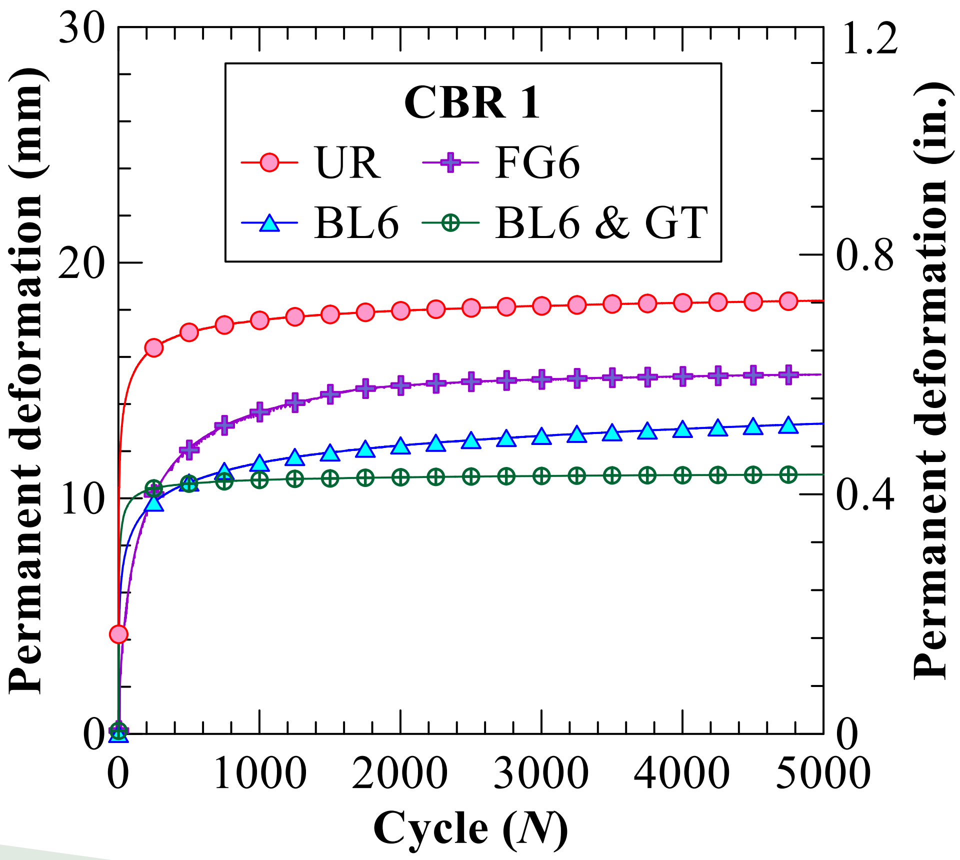

Results

Geocell (CBR = 1)

- ❑Permanent deformation (PD) with Geocell → reduction up to 4 times
- ❑3D Geocell vs 2D geogrids → 2.6 times reduction
- ❑PD of (3D Geocell + 2D geogrids) vs 3D Geocell → 5-10 % reduction

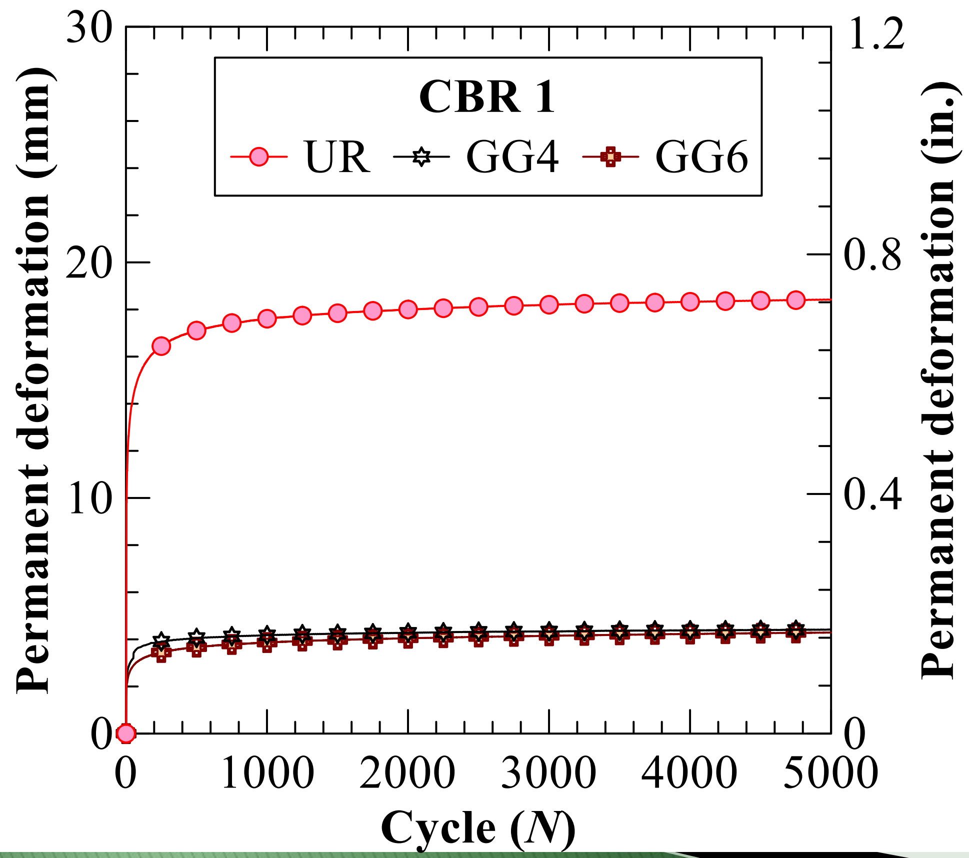

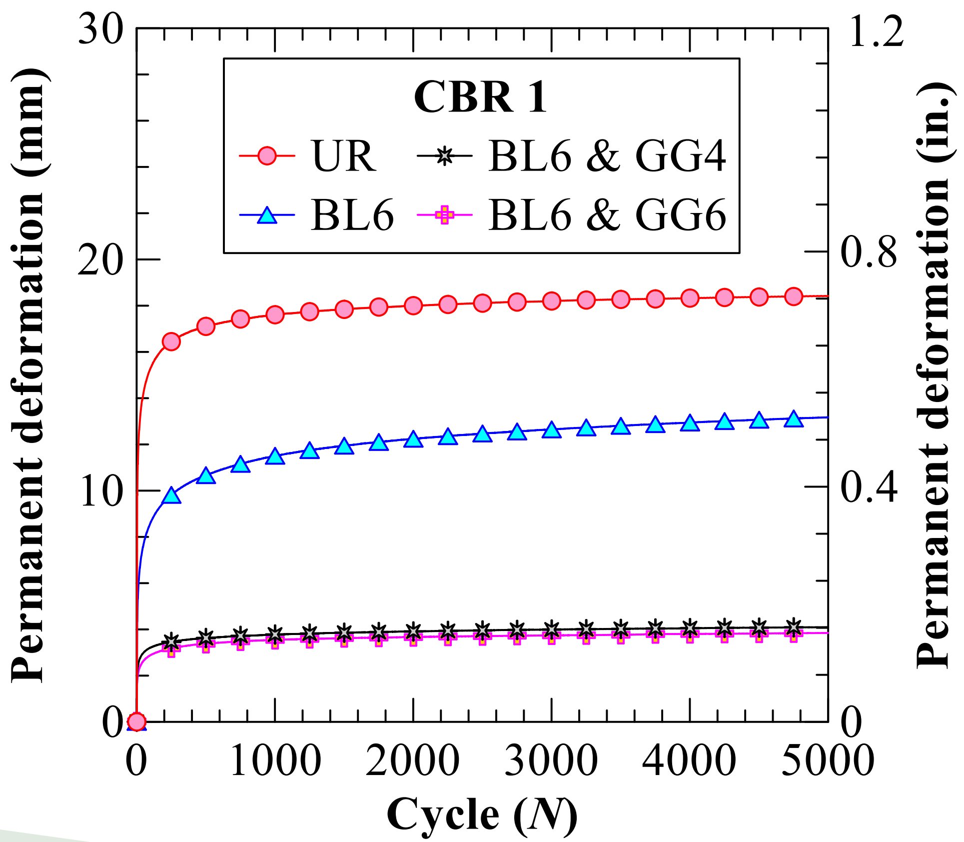

Results

Stress distribution angle CBR = 1

- ❑Vertical stress on subgrade reduced with geosynthetic reinforcement
- ❑Maximum vertical stress after 5000 cycles: BL5 > BL6 > BL7
- ❑Vertical stress values were used to determine stress distribution angles

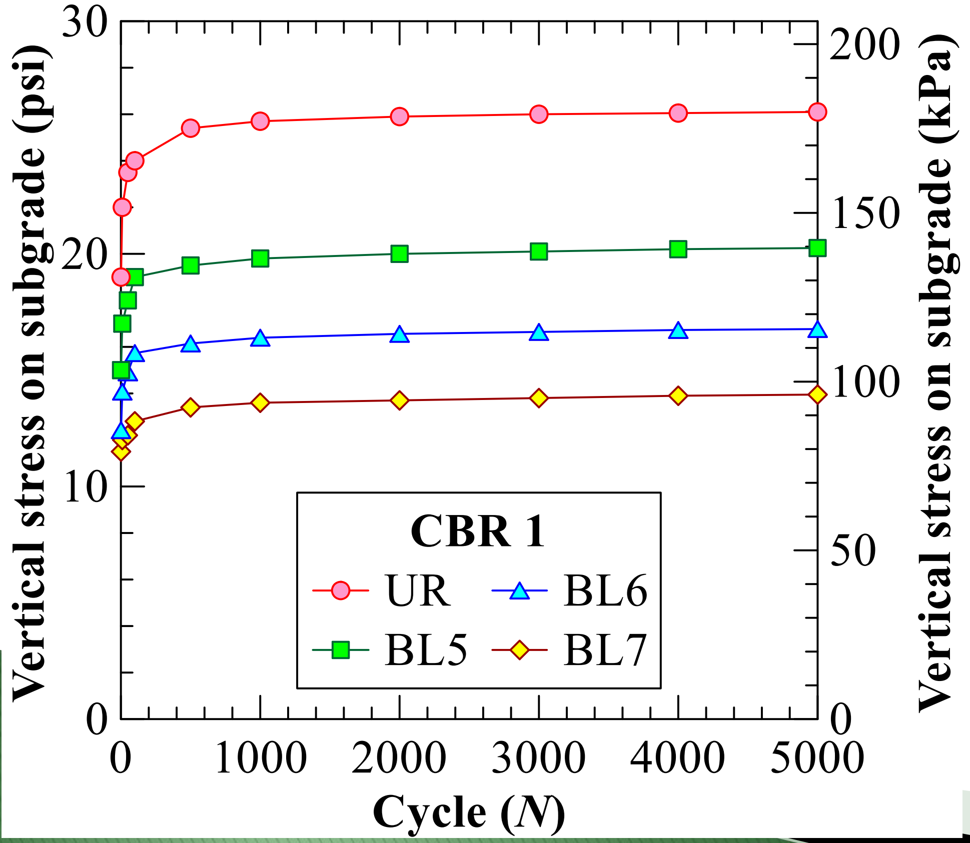

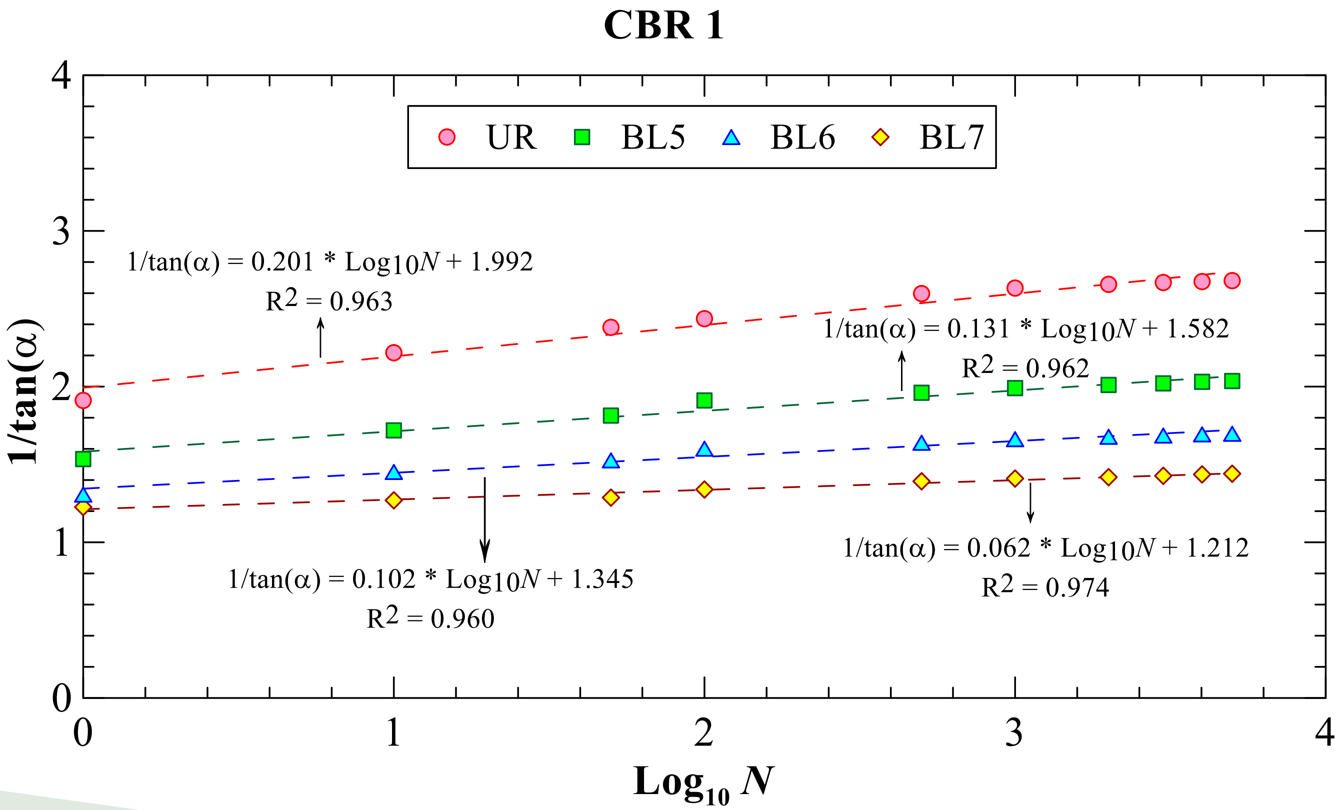

Results

Updated Design Parameters (geogrids only)

- ❑ **Stress distribution angle (α) showed the improvement with geogrids**
- ❑ α **decreases with the number of loading cycles**
- ❑ **New calibration equation is under development including λ and k functions**

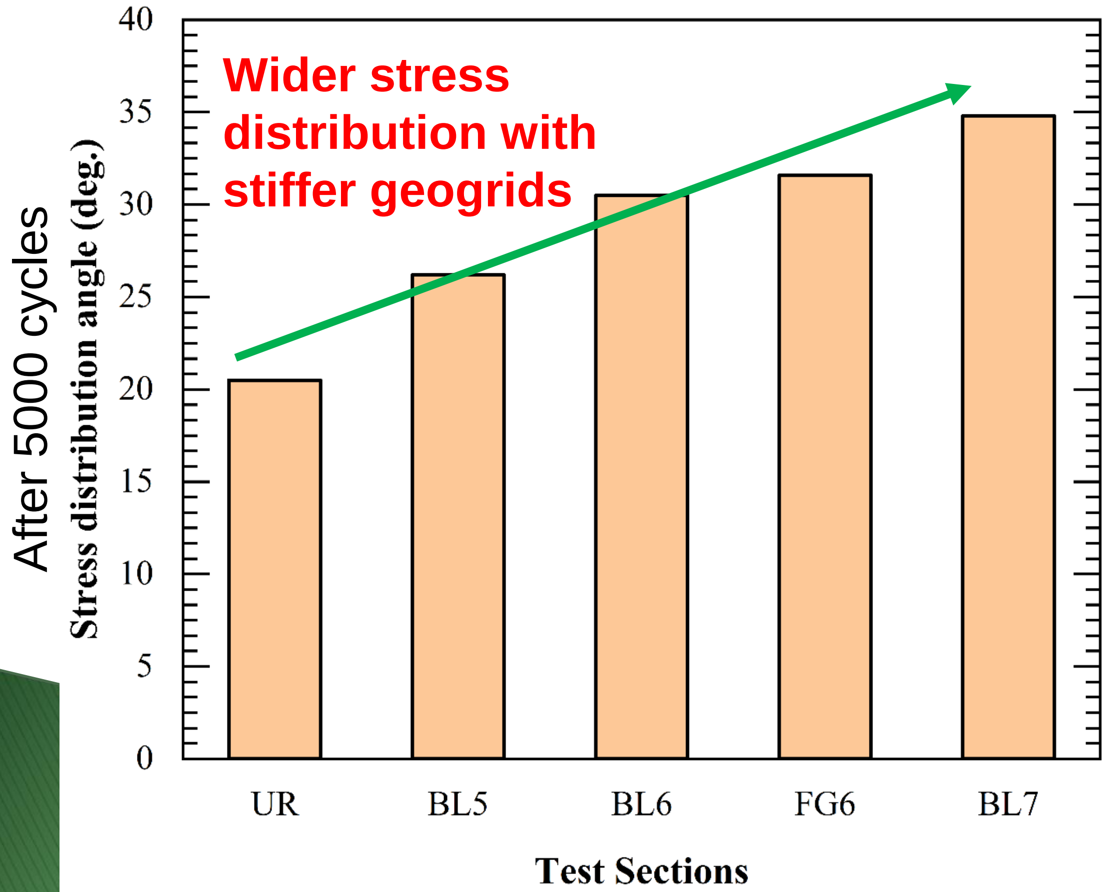

$$\frac{1}{\tan\alpha} = k + \lambda \log(N)$$

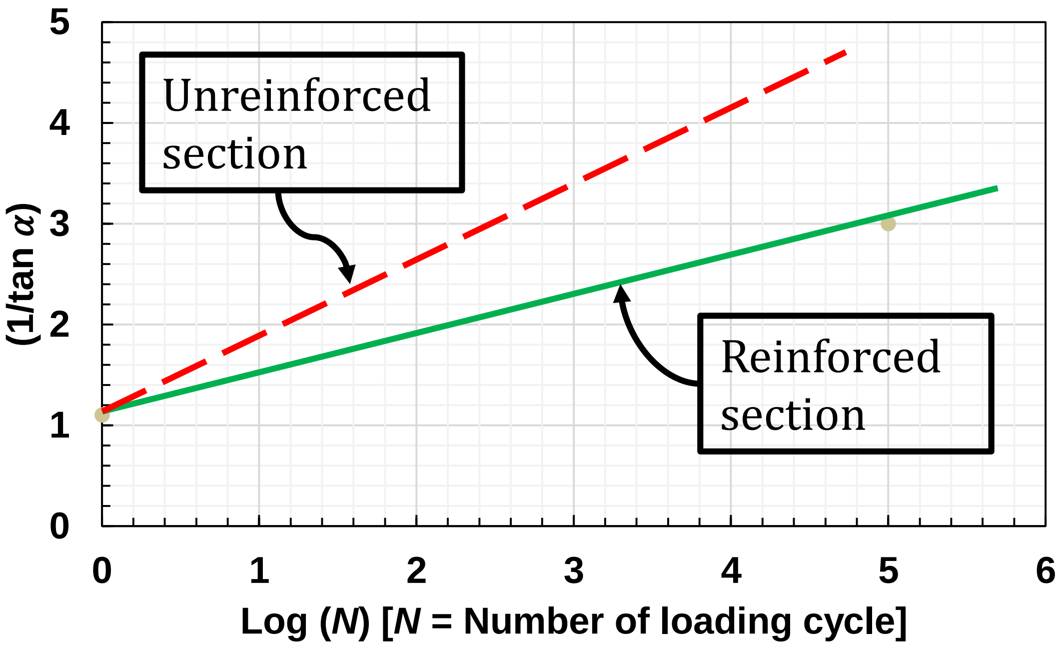

Typical plots of stress distribution angles (α) with number of loading cycle (N)

Results

Design Chart (under progress)

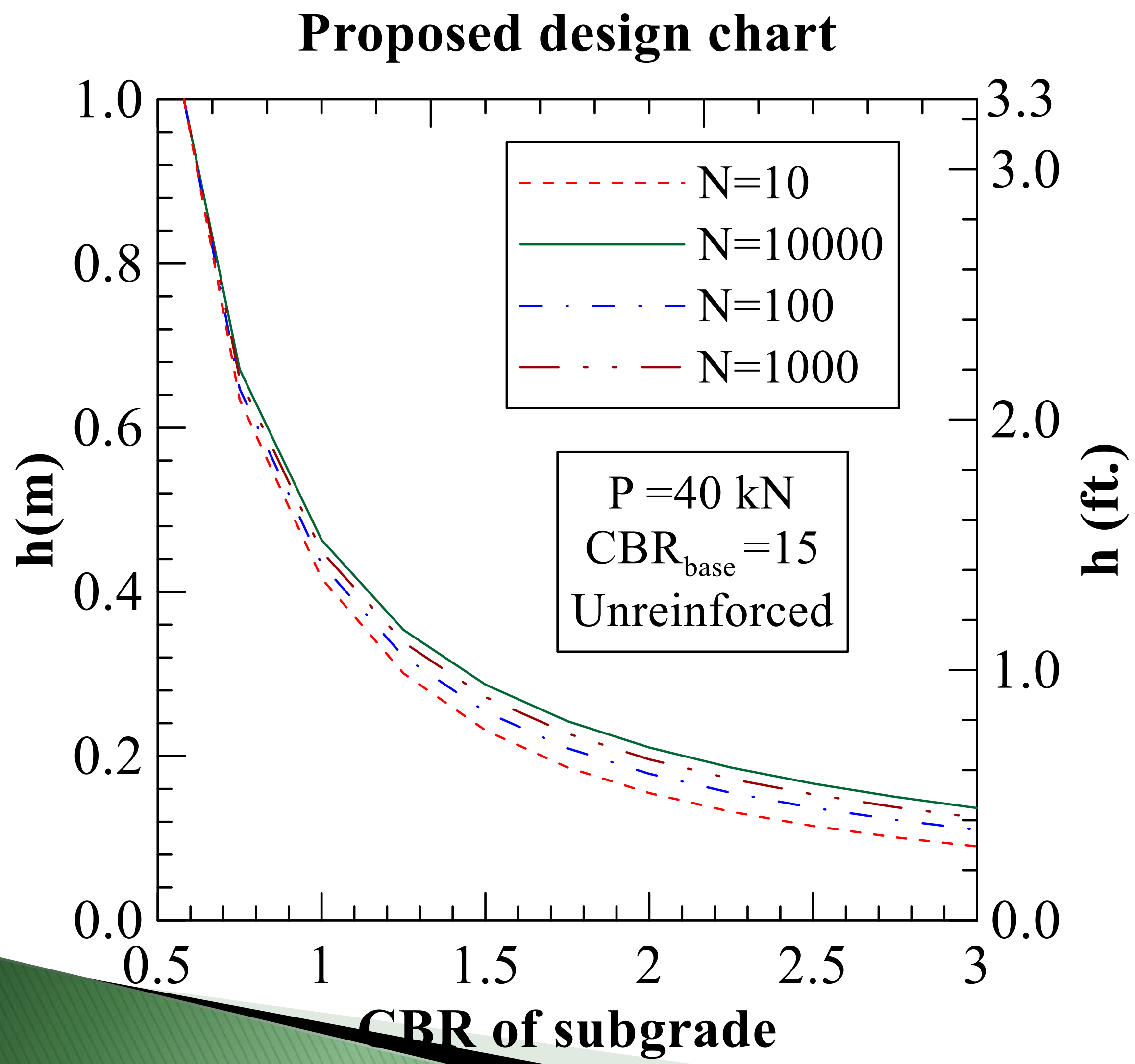

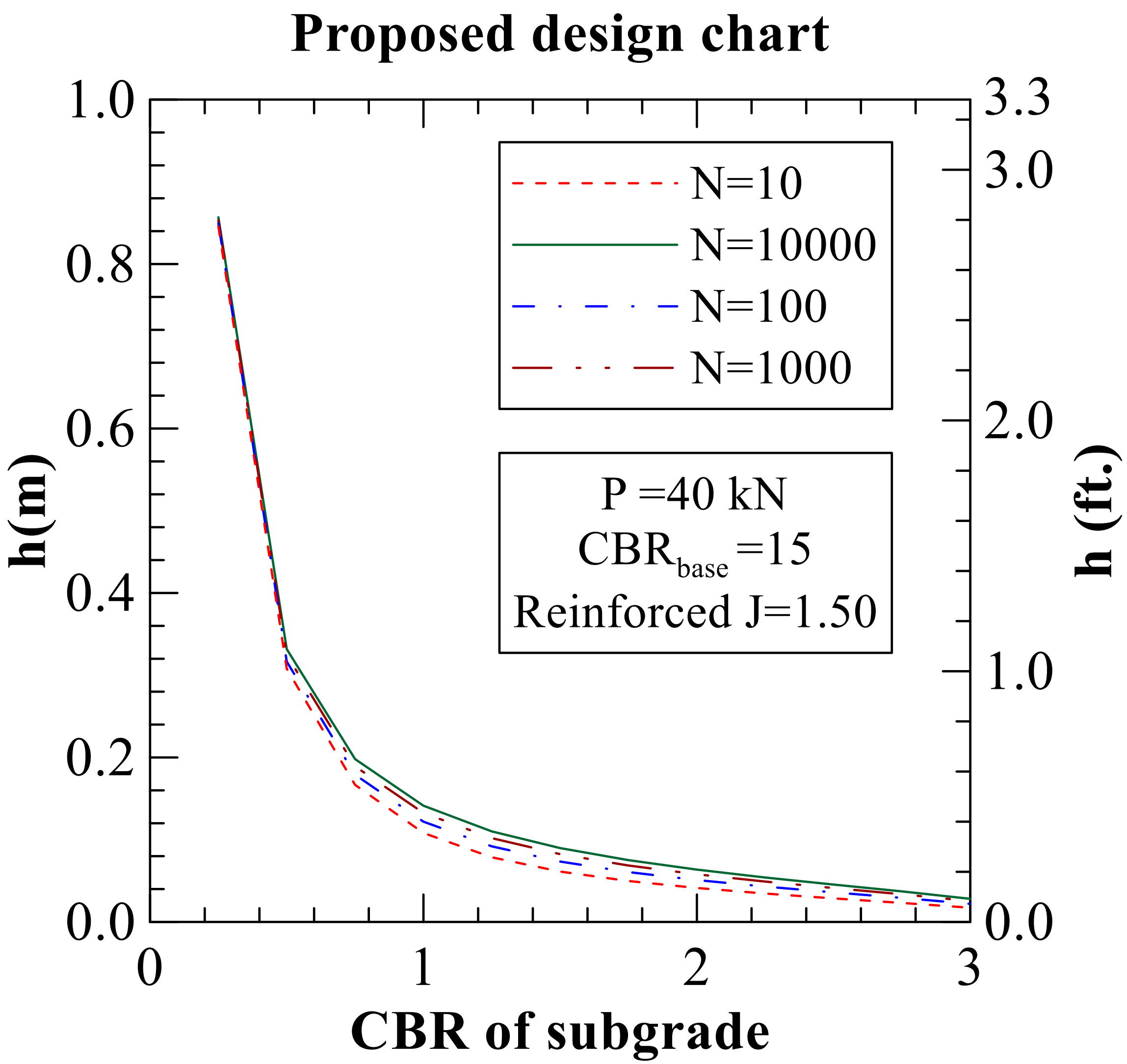

Summary

- **Geosynthetic reduced the vertical stress on subgrade by 20 to 50%**
- **Vertical stress distribution angle after 5000 cycles: UR < GG < GC < GG+GC**
- **For very soft soil, geogrid reinforced section reduced the permanent deformation (PD) by 1.5 to 2.0 times**
- **Geocell reinforced section reduced the PD by 3 to 4 times**
- **Inclusion of geogrid with geocell decreased the PD by only 5-10%**
- **G-H equation has been updated to include stiffer geogrids**
- **Design charts are now under development**

Future Scope

- ❑ **Need to validate the laboratory results with field study**
- ❑ **Currently collecting data from field- LWD, DCP, and VE-DCP**

Construction site in Louisiana, having very soft Subgrade. Geocell and Geogrids were used to enhance the foundation capacity

LIFE FORMS

Project: **Design and Testing of IFI Geosynthetic Products**

Number: **7**

Performance of pavement sections with H_2Ri geosynthetics

Project Leader: Nripojyoti Biswas

Team members: Md Ashrafuzzaman Khan and Krishneswar Ramineni

PI: Anand J. Puppala

Professor | A.P. and Florence Wiley Chair

Director – Center for Infrastructure Renewal

Closed Meeting

TAMU Site Proprietary

NSF IUCRC CICI TAMU SITE

NSF IUCRC CICI - IAB Fall 2022 Meeting

December 5-6, 2022

TEXAS A&M UNIVERSITY

Zachry Department of Civil & Environmental Engineering

Presentation Outline

- ❖ Introduction
- ❖ Task Plan
- ❖ Field Test Sections
- ❖ Falling-Weight Deflectometer Test & Results
- ❖ Life Cycle Analysis
  - ❑ Sustainability Analysis
- ❖ Conclusions
- ❖ Future works in other projects

Introduction

❖ Objective

- ❑ Evaluate the feasibility/efficiency of using H_2Ri geosynthetic for improving drainage and strength of pavement sections built on high-plastic expansive soil

- ❖ Field Studies indicated efficacy of application
- ❖ Laboratory studies
  - ❑ Control Section
  - ❑ Reinforced Sections

Control Section

Reinforced Section

Task Plan

Task 1

- ✓ Literature Review
- ✓ Geomaterial Characterization
- ✓ Construction of Test Sections
- ✓ Instrumentation and Monitoring

Task 2

- ✓ Laboratory Studies (H_2Ri)
- ✓ Wicking Tests
- ✓ Parametric Study

Task 3

- ✓ Life Cycle Analysis
- ✓ Carbon Footprint Analysis
- Design & Construction Guidelines

Field Test Sections

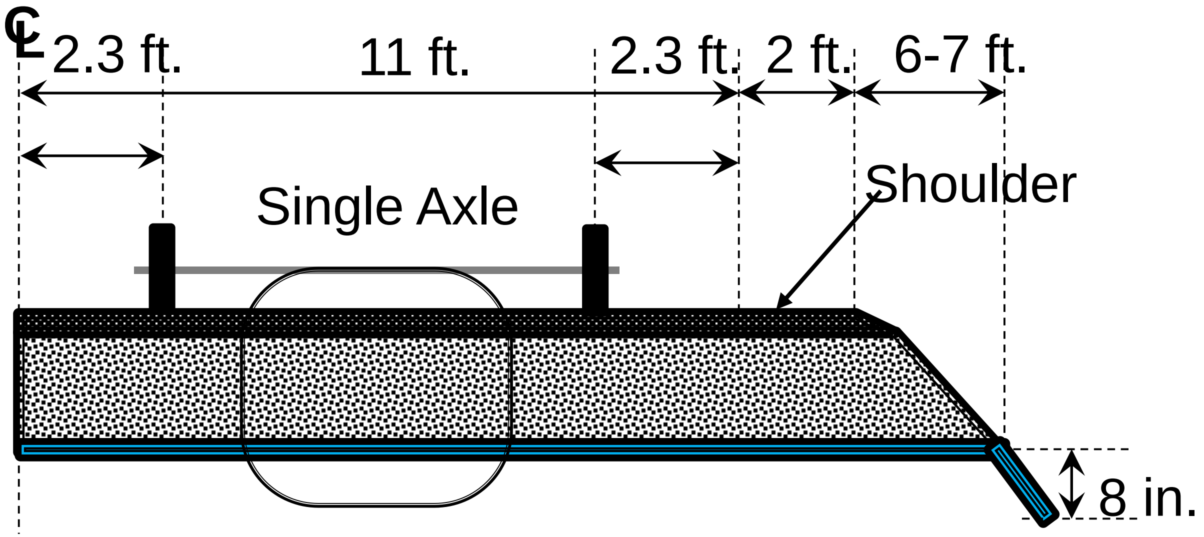

AC – Asphalt Concrete RAP - Reclaimed Asphalt Pavement Aggregates FB - Flex Base
EPC - Earth Pressure Cells SAA - Shape Array Sensors

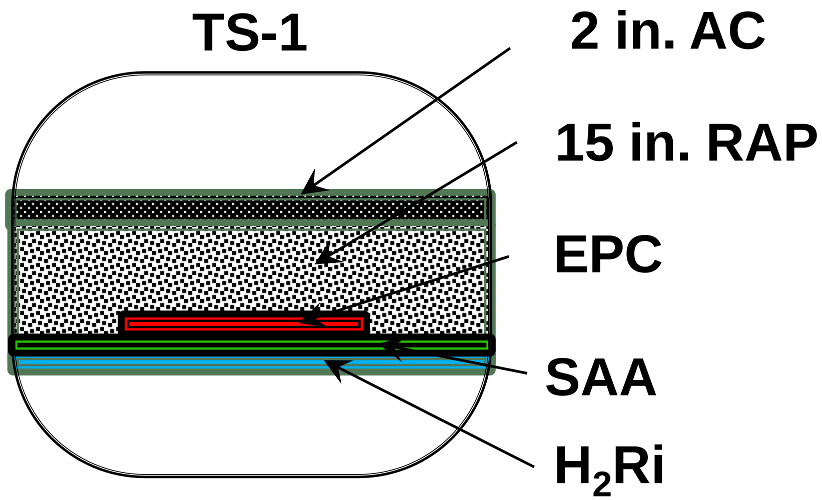

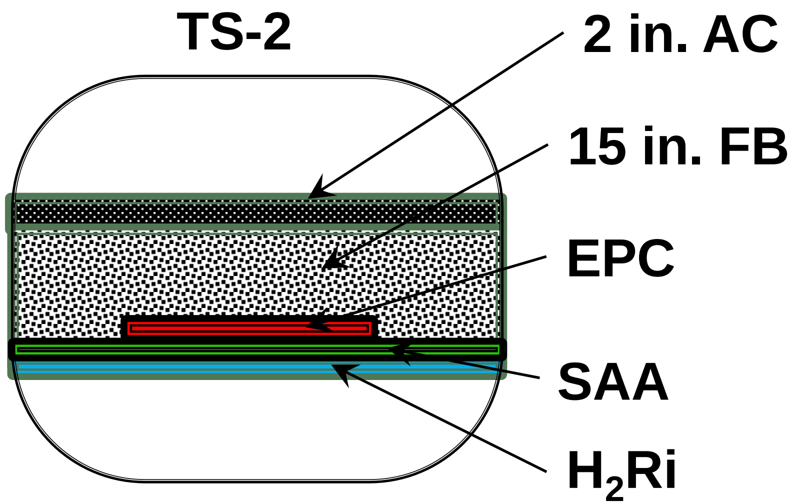

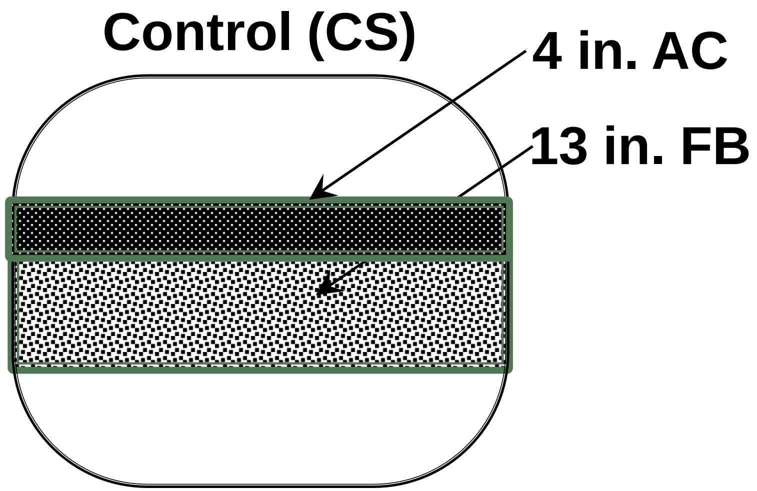

Falling Weight Deflectometer (FWD) Test

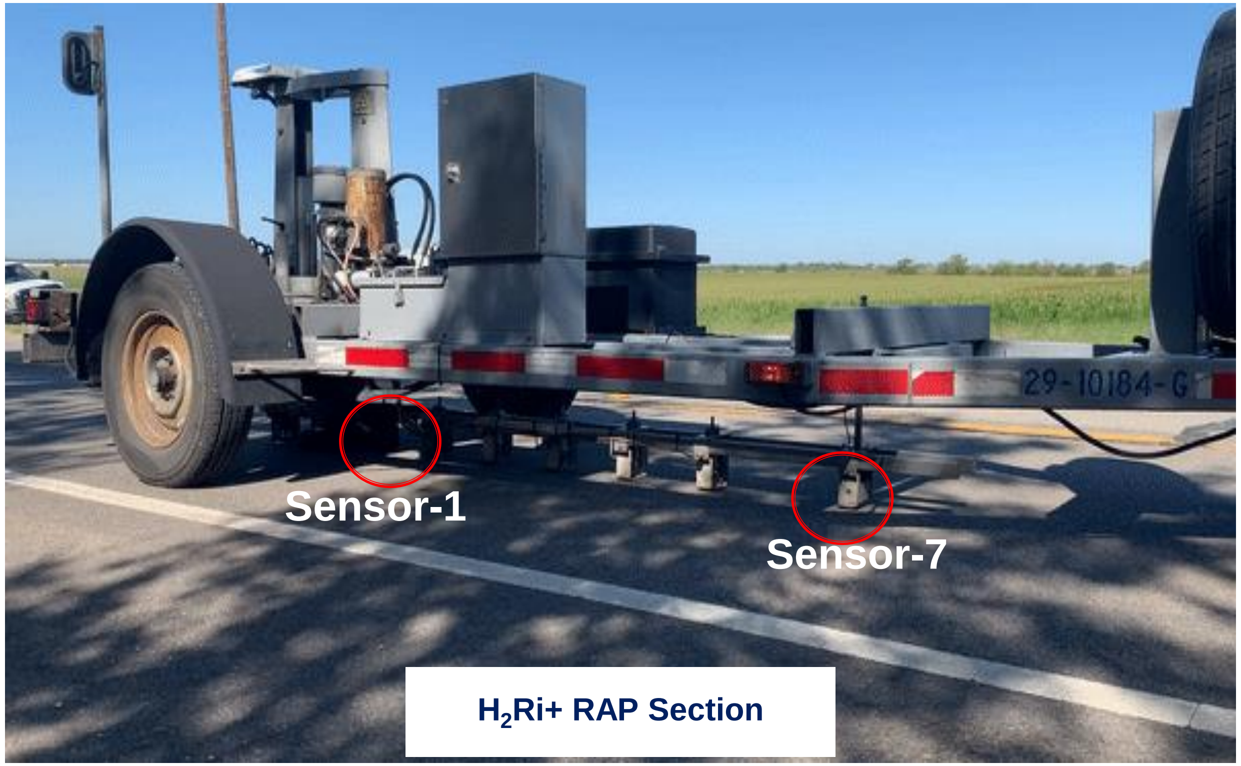

TS-1	**15 in. Reclaimed Asphalt Pavement (RAP) base + 2 in. Asphalt Concrete (AC) layer + H_2Ri geotextile**
TS-2	**15 in. Flex Base (FB) + 2 in. AC layer + H_2Ri geotextile**
CS	**13 in. FB + 4 in. AC layer**

Falling-Weight Deflectometer Test Results

- The performance indicators selected in this study were Base Layer Index (*BLI*), Lower Layer Index (*LLI*) and $AREA_{72}$

$$BLI = D_0 - D_{12}$$

$$LLI = D_{24} - D_{36}$$

$$AREA_{72} = 6\left(1 + 2\frac{D_{12}}{D_0} + 2\frac{D_{24}}{D_0} + 2\frac{D_{36}}{D_0} + 2\frac{D_{48}}{D_0} + 2\frac{D_{60}}{D_0} + \frac{D_{72}}{D_0}\right)$$

Note:
D_0, = Deflection sensor at 0 in.
D_{12} = Deflection sensor at 12 in.
D_{24} = Deflection sensor at 24 in.
D_{36} = Deflection sensor at 36 in.
D_{48} = Deflection sensor at 48 in.
D_{60} = Deflection sensor at 60 in.
D_{72} = Deflection sensor at 72 in.

Flexible pavement deflection bowl

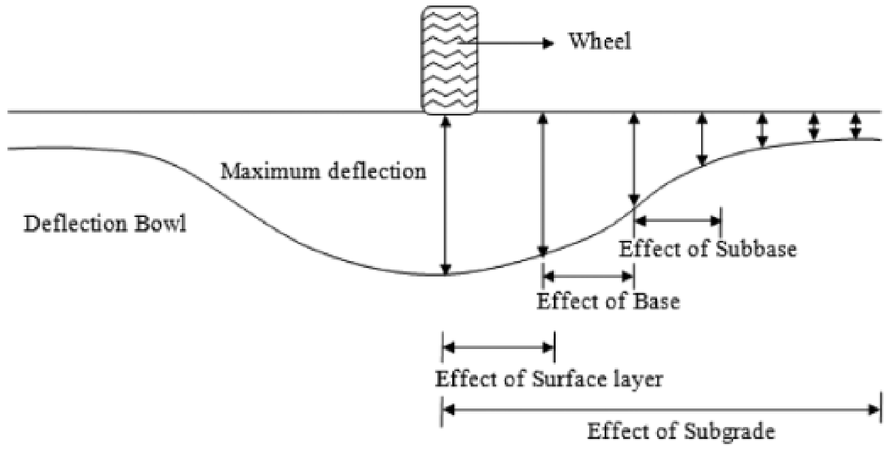

Falling-Weight Deflectometer Test Results

Section	Station	*BLI* (μm)			*LLI* (μm)			$AREA_{72}$ (in.)		
		2020	2021	2022	2020	2021	2022	2020	2021	2022
TS-1	1	135.6	171.7	194.1	53.0	50.0	53.8	26.2	23.9	23.6
	2	165.9	195.1	194.3	48.3	46.7	51.6	24.7	23.1	23.7
	3	160.1	181.1	189.4	48.5	48.5	52.2	24.6	23.3	23.9
	4	162.2	190.2	172.0	46.2	45.5	54.7	24.5	23.0	24.5
	5	150.7	185.7	228.6	45.7	47.2	71.0	25.0	23.2	22.8
	6	139.4	182.4	246.8	47.1	47.2	67.9	25.6	23.0	22.1
	7	180.7	230.1	248.5	58.9	56.9	78.4	23.9	21.8	22.2
TS-2	1	197.9	258.1	247.9	66.5	56.4	73.3	23.5	21.1	22.5
	2	206.2	256.3	249.7	70.5	62.2	63.1	23.1	21.2	22.0
	3	202.3	248.7	275.0	73.4	58.4	61.2	23.7	21.6	20.9
	4	191.3	230.9	220.9	63.4	53.1	69.2	23.7	21.9	23.0
	5	231.0	264.4	245.1	62.0	51.3	59.3	22.0	20.5	22.1
	6	208.4	215.4	207.3	90.7	57.4	56.3	23.1	22.4	22.6
CS	1	138.7	222.8	222.9	49.9	37.6	50.9	24.7	20.4	21.7
	2	133.9	207.5	216.7	41.0	36.1	48.9	24.4	20.6	21.5
	3	125.1	201.2	176.0	39.6	38.9	49.4	24.6	21.3	23.6
	4	105.5	185.9	161.4	42.3	51.3	57.7	27.2	22.5	24.7
	5	105.0	197.4	176.9	43.2	45.5	57.7	27.3	21.9	23.9
	6	126.7	187.2	163.6	45.7	41.7	52.5	25.7	22.4	24.6
	7	117.7	223.3	202.1	43.6	45.2	56.0	26.3	21.0	22.9

Sound Condition

BLI < 200 μm

LLI < 50 μm

Moderate Condition

200 μm < BLI < 400 μm

50 μm < LLI < 100 μm

- **RAP with wicking geotextile performing better than traditional flex-base material with wicking fibers**

Falling-Weight Deflectometer Test Results

Back calculated In-situ modulus and rut-life

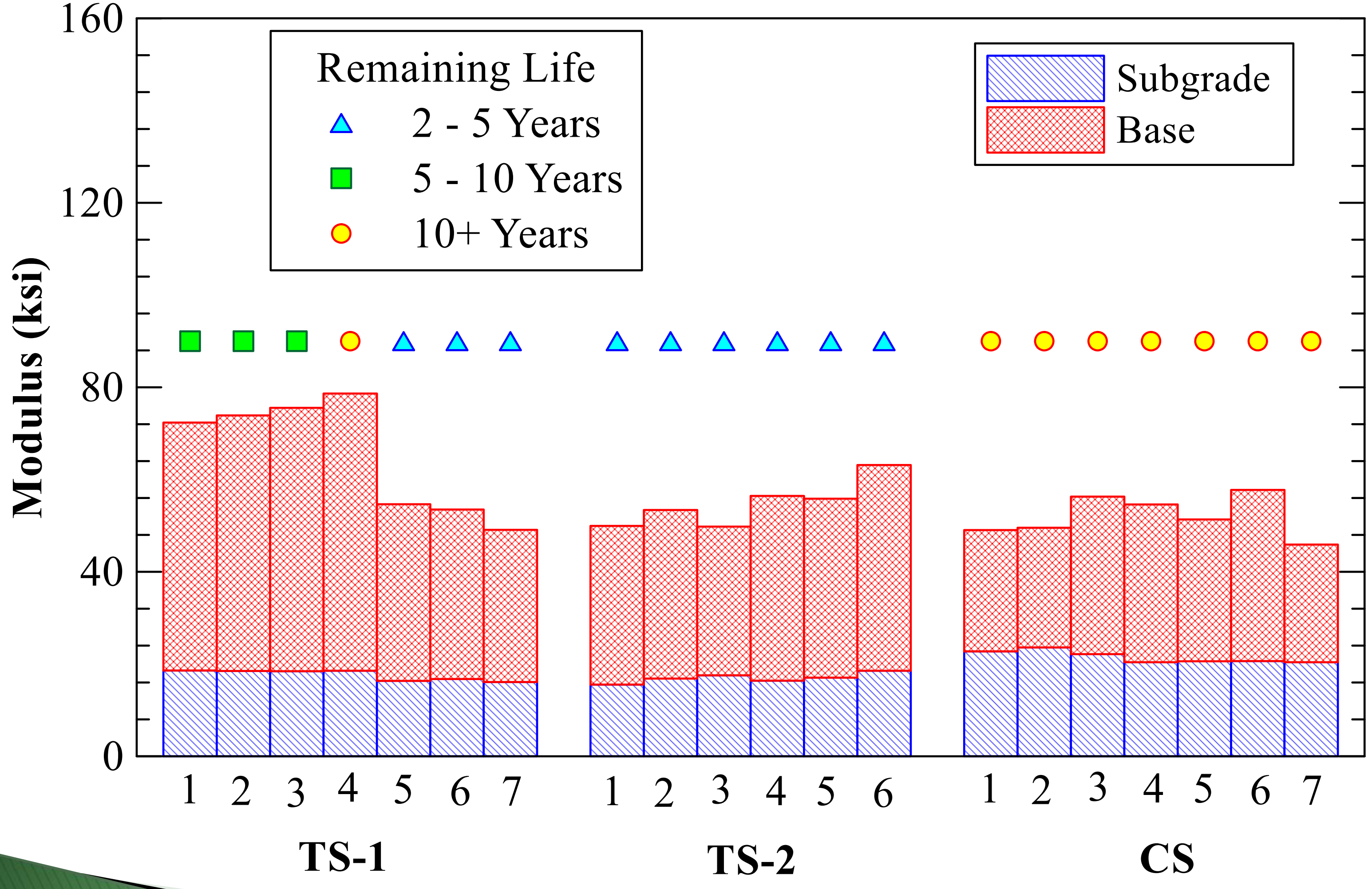

- ❖ Moduli values of subgrade layers (all sections) ≈ 15 – 20 ksi
- ❖ Moduli values of base layers (RAP) ≈ 45 ksi
- ❖ Moduli values of base layers (FB) ≈ 25 ksi
- ❖ Rut-life

  RAP > FB or Control

Life Cycle Analysis

Combined Assessment Framework (Das 2018)

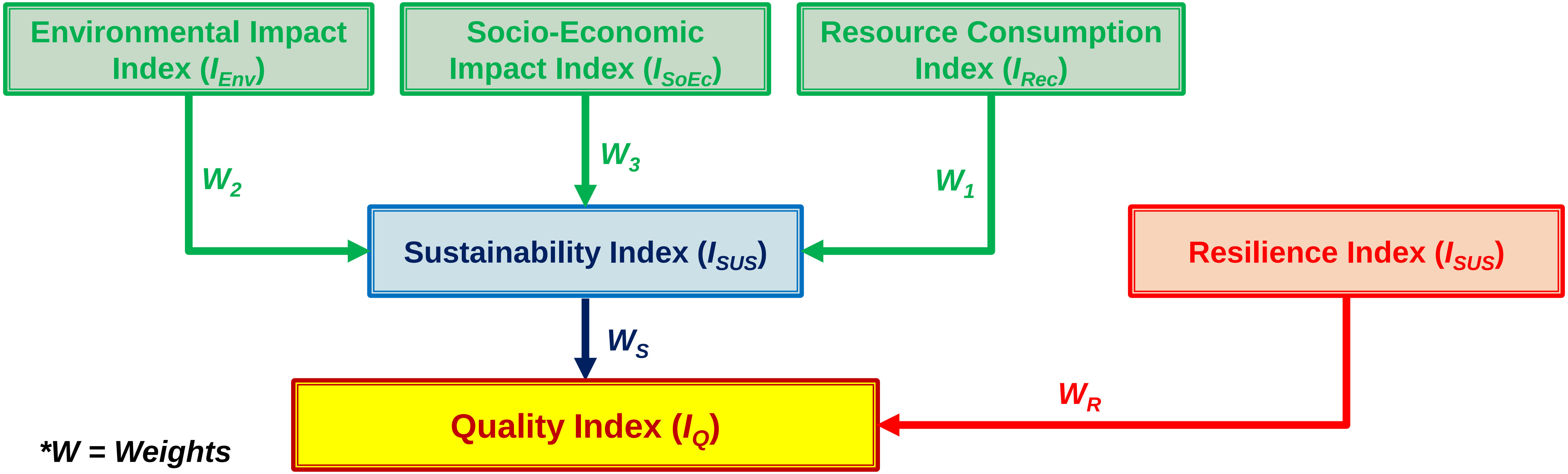

W = Weights

$*\sum W = 1$

$$I_{SUS} = W_1 \times I_{Env} + W_2 \times I_{SoEc} + W_3 \times I_{Rec}$$

$$I_Q = W_s \times I_{SUS} + W_R \times I_{Res}$$

Lower value indicates better alternative

Sustainability Analysis – Test Parameters

$$I_{Rec} = w_{1a} \times E_{E\ (material\ production)} + w_{1b} \times E_{E\ (Transportation)}$$

$$I_{Env} = w_2 \times GW_P$$

$$I_{SoEc} = w_3 \times C$$

Where,
w_i = Weight factors
E_E = Embodied Energy
GW_P = Global Warming Potential
C = Cost of the process

Test ID	A	B
Section ID	TS-1	Control
Section Parameters	15 in. RAP + 2 in. AC + H_2Ri gtx	13 in. FB + 4 in. AC
Section Length	130 ft.	130 ft.
Section Width	15 ft.	15 ft.

Sustainability Analysis – Database for Analysis

Database for Calculation

Material	Unit weight		Embodied energy (production) (MJ/kg)	GWP (kg $eqCO_2$/kg)	Cost (USD)		Transportation (miles)	Embodied energy (transportation) MJ/metric ton-km
RAP	122	pcf	0.074	0	$9.5	per ton	0	1.5
FB	135	pcf	0.083	0.0052	$12.6	per ton	20	
GTX	1.2	kg/m^2	77.7	2.37	$4900	15'x300' roll	100	
AC	145	pcf	5	0.086	$17	per ton	20	

Sustainability Analysis – Embodied Energy

$$I_{Rec} = w_{1a} \times E_{E\ (material\ production)} + w_{1b} \times E_{E\ (Transportation)}$$

Resource Category	Embodied Energy (MJ)		Consumption of Embodied Energy (%)			Weighted Resource Use	
	A	B	A	B	Weights	A	B
Production	298842.0	224446.5	57.1	42.9	0.5	28.6	21.4
Transportation	2823.6	18213.0	13.4	86.6	0.5	6.7	43.3
					I_{Rec}	35.3	64.7

- RAP with wicking geotextile has lower Embodied Energy as compared to traditional section

Sustainability Analysis – Environmental Impact

$$I_{Env} = w_2 \times GW_P$$

Environmental Impact Category	Emission Category Contribution		Contribution to Emission Category (%)			Weighted Environmental Impact	
	A	B	A	B	Weights	A	B
Global warming potential: $kgCO_2e$	7383.7	5158.8	58.9	41.1	1.0	58.9	41.1
					I_{Env}	58.9	41.1

- RAP with wicking geotextile has higher kg eq. of CO_2 emission as compared to traditional section

Sustainability Analysis – Socio-Economic Impact

$$I_{SoEc} = w_3 \times C$$

Socio-economic Impact Category	Cost Category Contribution		Contribution to Cost Category (%)			Weighted Environmental Impact	
	A	B	A	B	Weights	A	B
Cost of Treatment: USD	3927.5	2595.0	60.2	39.8	1.0	60.2	39.8
					I_{SoEc}	60.2	39.8

- ❖ RAP with wicking geotextile has higher cost of implementation as compared to traditional section

Sustainability Analysis

$$I_{SUS} = W_1 \times I_{Env} + W_2 \times I_{SoEc} + W_3 \times I_{Rec}$$

Section ID	A	B	Weights	A	B
	(1)	(2)	(3)	(4)=(3)*(1)	(5)=(3)*(2)
Resource consumption index, I_{Rec}	35.3	64.7	0.3	11.6	21.4
Environmental impact, I_{Env}	58.9	41.1	0.3	19.4	13.6
Socio-economic index, I_{SoEc}	60.2	39.8	0.3	19.9	13.1
		Sustainability index	I_{sus}	50.9	48.1

❖ RAP with wicking geotextile is marginally less sustainable as compared to traditional section

Conclusions

- Falling-weight deflectometer studies indicate that RAP+H_2Ri section performance is comparable to Control Section
- This corroborates results from APLT tests and in-situ monitoring results (Dec 2021 meeting)
- Benefits of application of the novel studies were verified using laboratory studies (May 2022 meeting)
- Sustainability assessment indicates GHG emissions during production of geotextile and cost of geotextile are major factors affecting sustainability benefits of the project
- Future benefits could be realized with the inclusion of Resiliency Function

Future Works in Other Projects

Field Construction

Length of the section- 250′

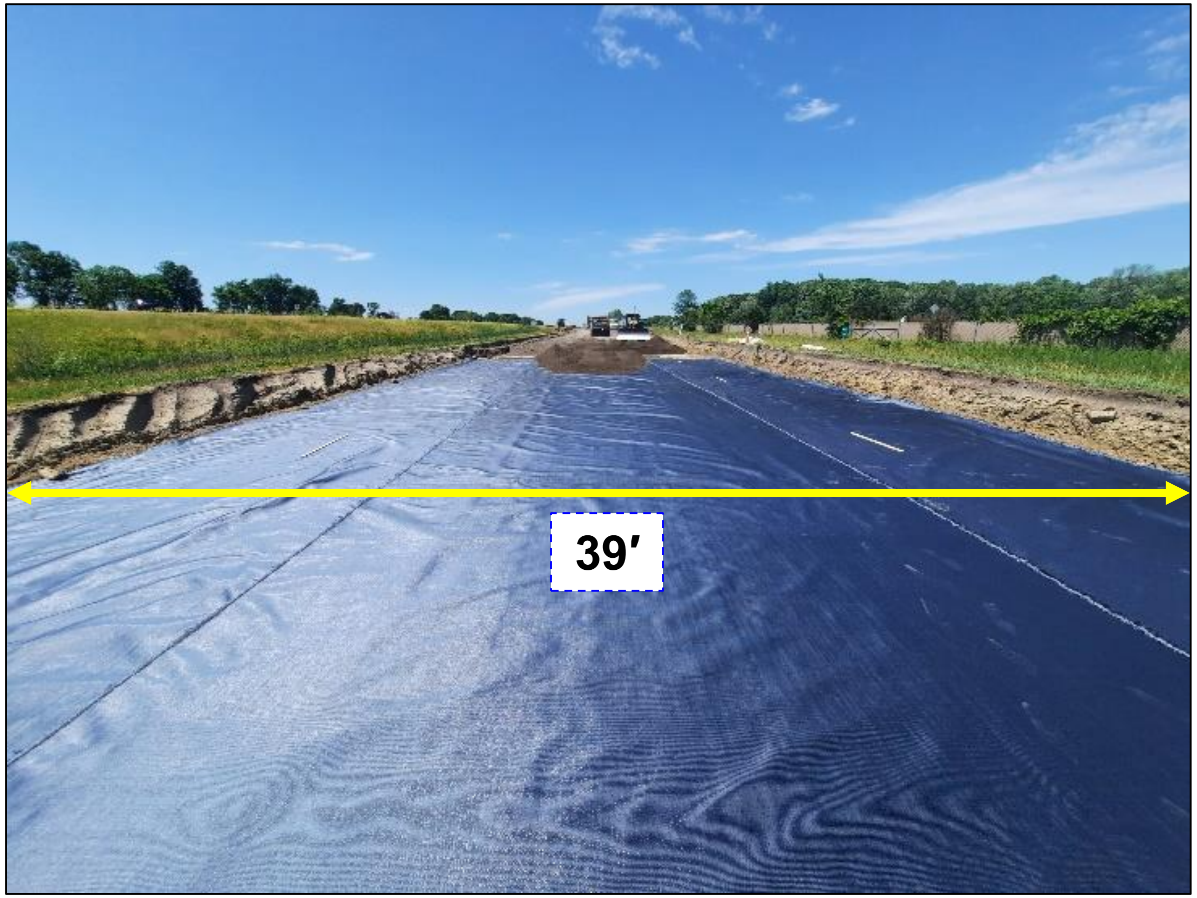

Installation of Wicking geotextile at the interface of subgrade and subbase

Slide Courtesy: Dr. Bora Cetin, MSU

Field Construction

Trenches at the shoulder

Slide Courtesy: Dr. Bora Cetin, MSU

Field Construction

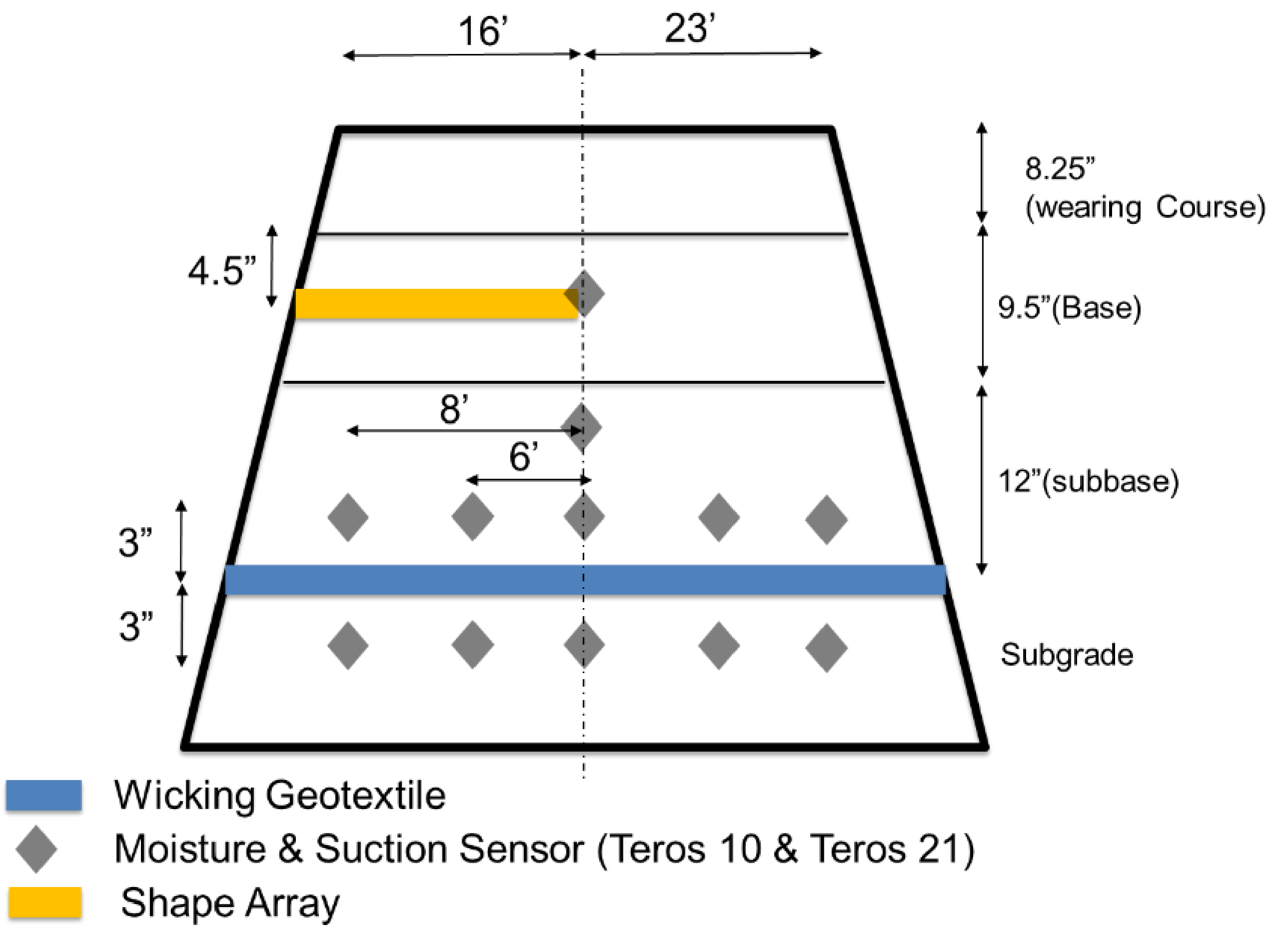

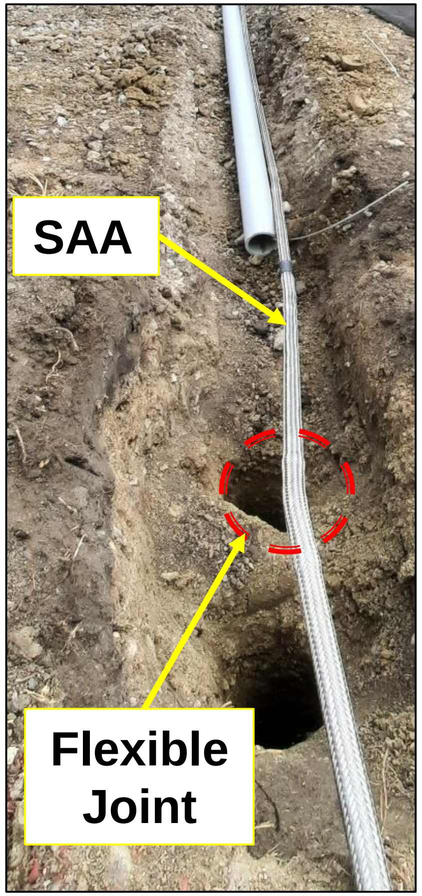

Sensor Installation

Slide Courtesy: Dr. Bora Cetin, MSU

LIFE FORMS

Project: **Performance of pavement sections with H_2Ri geosynthetics**

Number: **8**